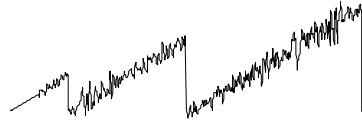NEES at CU Boulder

01000110 01001000 01010100

The George E Brown, Jr. Network for Earthquake Engineering Simulation

Fast Hybrid Testing at CU NEES:

Benchmark Tests

By

Eric Stauffer
Gary Haussmann
Katherine Smith
Robb Wallen

(Intentionally Blank)

FOREWORD

Hybrid simulation has received much attention lately, within the NEES community and internationally.

Until fairly recently emphasis (within the NEES community) was on distributed hybrid simulation, yet our research community is slowly realizing that fast or real time hybrid simulation has a major role to play in earthquake engineering simulation[1].

A recent NSF site visit to our site requested that we report in more ample details validation tests performed in 2003. We took this as a challenge to go beyond NSF requirements, and to undertake a full battery of validation tests to highlight capabilities and limitations in real time hybrid simulation at our site.

This effort was lead by Dr. E. Stauffer (who performed a superb job under tight time constraint), our former Technical Director, in collaboration with CU-NEES CO-PI and staff.

The following report is, in my humble opinion, a major milestone in real time hybrid simulation as it provides both a template and a metric. Other sites may want to espouse the former, adapt it to their facilities, and ultimately improve it.

With a template, or shall we say a Standard for Real Time Hybrid Validation (SRTHV in NEESinc parlance), we would have a rational means of assessing various capabilities.

My sincere thanks to Eric and CU-NEES.

Victor Saouma
CU-NEES PI and Director

Boulder, Nov. 2007

---

[1] Workshop on Simulation Development organized by NEESinc in Chicago, Sept. 13, 2007.

(Intentionally Blank)

Table of Contents

List of Figures

1 Executive Summary

Hybrid simulation has benefited from increasing attention as a viable and economical means for conducting earthquake engineering research. This is likely in part due to the practical and intellectual appeal of taking a complex and/or large problem and reducing to more manageable components one or more of which are sufficiently will understood to be represented with existing computer modeling techniques. And the remainder, owing to uncertainties or other considerations, is represented physically in the laboratory and tested. These distinct components remain an integrated whole or a so called hybrid model that is the subject of either realtime or distorted time simulations. The distortion of time during a hybrid earthquake simulation has significant implications that limit the scope of work that can be carried out under such conditions. Most fundamentally is the limitation that the component(s) subject to physical testing behave in a rate or velocity independent manner.

Realtime hybrid simulation directly addresses this limitation very simply by accurately representing time in the simulated event. In doing so many of the assumptions that are the basis for time distorted hybrid simulations are no longer valid and additionally new technical challenges arise. The Fast Hybrid Testing facility at the University of Colorado has developed and continues to enhance and innovate a realtime hybrid simulation methodology that broadens the scope of possible work to include devices and materials that are rate sensitive. In this report the methodology is applied to two distinct research applications establishing:

· The CU hybrid testing laboratory currently has a 3 degree of freedom limitation for the experimental test component.

· The computational limitation of realtime hybrid testing is model dependant with the current demonstrated limit in the range of 130 degrees of freedom.

· The platform developed for realtime hybrid simulation is flexible and expandable both in terms of what can be tested in the lab as well as what can be simulated within the computer.

· The system level challenges of implementing and applying this technique have to a very large degree been successfully completed.

· A variety of benchmark results have been established demonstrating a high level accuracy and versatility.

2 Abstract

The University of Colorado (CU) Fast Hybrid Testing (FHT) facility utilizes a customized and unconditionally stable implicit time integration technique to combine numerical modeling and an experimental substructure into a unified hard realtime earthquake simulation. Initially the FHT system was designed, developed and commissioned with the understanding that the experimental test component would behave as a structural component, which is to say that it would react to an imposed displacement history at its boundary with a corresponding force history. This assumption is fundamental to the original development of the implicit time integration algorithm and most other hybrid simulation algorithms. To view a rate sensitive device, such as the MagnetoRheological (MR) dampers recently tested at the CU NEES facility, as such a structural component is to misrepresent the true mechanical nature of this device. Indeed, based on existing system identification test data, such a damping device is more accurately represented as a component which reacts to an imposed velocity history at its boundary with a corresponding force history. This understanding has made it necessary to generalize the formulation of the displacement based implicit time integration algorithm so as to correctly accommodate the velocity based nature of a device such as an MR Damper. The benchmark tests presented in this report are intended to provide a better understanding of the newly implemented damper compatible hybrid integration algorithm in terms of measurable performance data. This data will serve to establish the necessity, capabilities and limitations of a hard realtime FHT system using the new generalized formulation, in addition to identifying areas which need further work or refinement to improve this testing technology. Advances such as this play an important role in the technical development and future of hybrid testing.

3 Background

This report summarizes the capabilities, limitation and some of the recent advances of the hybrid testing capabilities of the University of Colorado (CU) Fast Hybrid Testing (FHT) facility, an equipment site member of the Network of Earthquake Engineering Simulation (NEES). Two different types of Real Time (RT) hybrid simulations are used to establish performance benchmark results which other hybrid testing facilities can use for comparison purposes and interested researchers can use to develop a working understanding of the requirements and needs of RT hybrid testing.

In the early part of 2005 the equipment development phase at the CU NEES facility was concluded with a series of RT tests carried out on a relatively simple steel frame hybrid structure. Consistent with the type of hybrid testing that has been done for many years, a structural element was the experimental component off the hybrid model. The final test in this series involved strong nonlinear behavior in both the physical/experimental

portion of the structure and the numerical /Finite Element (FE) portion. These simulations will act as the first part of the two types of benchmark tests.

More recently nonlinear damping devices, Magneto-Rheological (MR) dampers, have been tested to evaluate there potential as semi-active earthquake damage mitigation devices. A series of tests have been conducted to verify and evaluate hybrid simulations involving these highly nonlinear damping devices. In order to complete these tests the direct time integration algorithm used at CU NEES was generalized, allowing for the participation of an experimental test element with nonlinear damping properties. These tests are the second part of the benchmark results.

Several terms will be used throughout this report that will now be defined in an effort to promote a more clear understanding of there use as applied to hybrid simulations. First, the term realtime has been used rather loosely in many circles and has caused some confusion within the hybrid simulation community. For our purposes realtime is defined in the same way as computer scientist define the term *hard realtime*. The following definition will be adapted here and is taken from Wikipedia the online encyclopedia. "A system is said to be **real-time** if the total correctness of an operation depends not only upon its logical correctness, but also upon the time in which it is performed. The classical conception is that in a **hard** or **immediate real-time system**, the completion of an operation after its deadline is considered useless - ultimately, this may lead to a critical failure of the complete system." As a researcher working with rate sensitive materials and/or devices such a strict definition provides assurance that the importance of velocity in a hybrid simulation will be fully honored.

Hybrid models may be divided into two distinct conceptual components. One which will be physically tested in the laboratory and will be designated the *experimental component*, while the remaining portion of a model will reside in some form of mathematical representation and will be designated the *numerical component*. These two components combine to makeup the *hybrid model* or structure.

Returning to the notion of time it will be helpful to define three additional terms involving time. *Prototype time* corresponds to passage of time during some usually recorded event such as the famous El Centro earthquake on May 18th 1940 in the Imperial Valley of California. *Simulation time* is the marking of time within a computer simulation and may or may not relate coherently to the passage of time as marked by a clock on the wall. Typical direct time integration techniques establish equilibrium at discrete intervals of *simulation time* that are Δt seconds apart. *Testing time* is the marking of the passage of time during, in our case, a hybrid simulation and can be thought of as the clock on the laboratory wall. Given a consistent starting point and that all three definitions of time are equivalent over the widest possible range of time intervals we have hard realtime conditions.

Materials and devices which are *rate sensitive* play a critical roll in the importance of realtime hybrid testing. A device or material is said to be rate sensitive if the response is dependant on the rate of loading or deformation. A good example of a nonlinear rate

sensitive device is a police officer at work issuing speeding tickets. The officer is not concerned about a car's position or displacement but is very sensitive to a cars velocity. Based on the input the officer receives, which is an approximate velocity measurement, the officers output will either be nothing (for cars not exceeding the speed limit) or a speeding ticket that is in some way proportional to the amount the car is exceeding the speed limit.

4 Introduction

Seismic performance evaluation of structures may be carried out in a wide variety of ways. Shaketable testing is perhaps the most obvious, straightforward technique and involves placing a full size or scale model of a structure on a shaketable and subjecting it to earthquake motion. This type of testing is effective but limited by the size of a structure that may be tested owing to the cost of both the test specimen and the potentially large shaking table. Another method, Pseudo-dynamic testing, attempts to simulate the conditions of an earthquake by fixing the base of the structure and imparting motion and forces to the structure at carefully selected points. The imparted motion is determined by the direct integration of the governing Equations of Motion (EOM) for the full test structure. RT pseudo-dynamic tests occur when there is a one to one correspondence between the prototype time, simulation time and testing time. Some economy may be achieved by dividing the test structure into a physical component and an analytical component creating a hybrid structure. Only the physical substructure needs to be constructed and tested in the laboratory while the remaining analytical substructure is modeled within a computer typically, using finite element methods.

5 System and Component Level Performance Considerations

A tightly integrated system of networked computers, high-performance hydraulic equipment, controls, custom modeling and data acquisition software are all critical components to the CU NEES FHT system. A bottle-neck at any one of these components will compromise the effectiveness of the overall system. With this in mind the system has been designed in a modular way such that individual components can be added or upgraded without being forced to redesign the system or replace other major components.

5.1 Realtime Network

The communication backbone of the system is a realtime fiber-optic shared memory network called ScramNet. This network replicates a 2 M-byte segment of memory in all of the network nodes. Each host processor on the network maps the shared memory segment into its read/write RAM providing a deterministic high-speed communication network ideally suited for hybrid testing. The network can be expanded to include up to

256 nodes or processors and a wide variety of computer bus form factors are supported. A schematic representation of the network is illustrated in Figure 1.
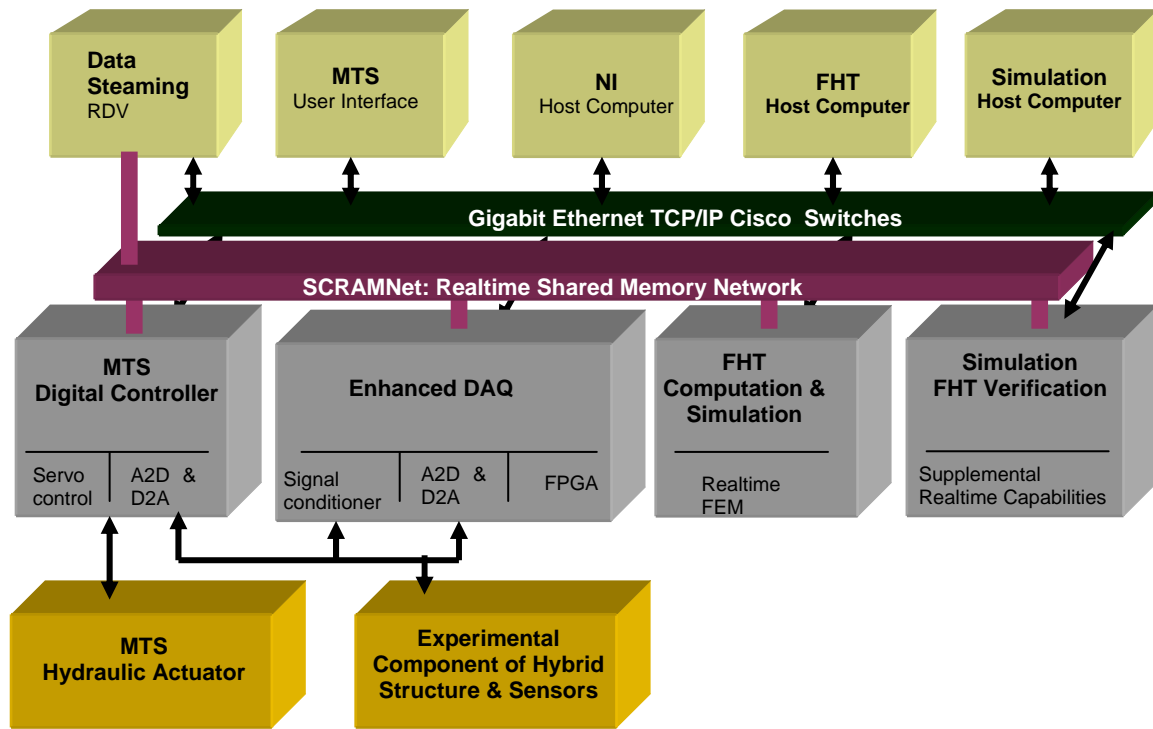
Figure 1: System Component Overview

The MTS Digital Controller acts as the central controlling component in the network by providing a network interrupt every 1/1024 seconds that keeps the clock cycle for each of the other RT components synchronized. This component also provides the user configurable controls to drive each of the systems three hydraulic actuators and uses a portion of the shared memory for control and data acquisition purposes.

5.2 Data Acquisition

It has proven to be beneficial to have the components of a system such as this in a distributed network like the one shown in Figure 3.1. The principle of divide and conquer has many obvious benefits but also creates some interesting challenges especially in the area of data acquisition. Fundamentally there are two distinct sources for test data; 1) Data from the Finite Element Model (FEM) including relevant convergence information resulting from the solution of a complex system of nonlinear equations and 2) data from the experimental component including actuator controls. In order to acquire and synchronize data from these two sources, in realtime, an Enhanced DAQ system has been developed at CU NEES[1]. This enhanced system expands the

transducer channel count for the system and collects, in one location, the data from both the experimental and computational components of the simulation.

5.3 FHT Computation and Simulation

At the heart of the FHT system is a computation and simulation computer that runs a customized FEM program that integrates conventional finite elements (structural elements such a beams and trusses) with hybrid testing elements (in which nodal forces and displacements are measured and controlled respectively, not computed). This FEM program (currently, OpenSEES) has been modified to run under a realtime Operating System (OS) which provides a highly deterministic computational environment. A conventional direct time integration algorithm used for dynamic seismic simulations has been modified, or more precisely constrained, for realtime hybrid simulations. An adaptation of the implicit integration scheme of Hilber, Hughes and Taylor is has proven to be a relatively robust and stable for FHT.

5.4 MTS Controller and Hydraulic Equipment

The experimental component in a FHT must be precisely and reliably controlled throughout a hybrid simulation. Additionally, safety is an important consideration and limits and/or interlock conditions need to be established and implemented during simulations. The hydraulic testing equipment, controls and data acquisition provided by MTS Systems Corp. play a very critical and central roll in hybrid simulations.

Each control cycle of the MTS digital controller concludes when the control and experiment transducer signals are updated on the ScramNet. Upon writing the last of these updated signals a network interrupt is generated and communicated throughout the shared memory network. This interrupt initiates a new clock cycle for each of the realtime components in the distributed network shown in Figure 3.1. This interrupt is generated at a rate of 1024 Hertz and imposes a very important constraint on the direct time integration routines that are used in hybrid testing.

5.5 Data Streaming

The remaining component on the RT network provides background functions such as data streaming capabilities that enhance a remote observer's testing experience. These capabilities are nonessential to a RT hybrid simulation and are part of the NEES grid software that is provided and supported by NEES IT. Efforts continue at NEES IT to provide and support some networking capabilities and software for nonrealtime hybrid simulation capabilities. A lack of execution determinism and network latencies make geographically distributed realtime hybrid simulation unrealistic at the present time.

5.6 Computational Constraints

Simulations conducted in hard realtime necessitate that a limit be placed on the amount time allowed to compute equilibrium at each time step. An unconditional stable (for linear models) implicit direct time integration algorithm has been adopted at CU NEES. Two supplemental constraints are imposed on the conventional algorithm of Hilber, Hughes and Taylor. By fixing the number of Newton iterations as well as the amount of time allowed for the computation at each iteration the algorithm is rendered deterministic with respect to execution time. Both of these constraints have far reaching implications but are essential. The computation time for a single Newton iteration is established by the master clock cycle of the MTS controller mentioned above and is 977 micro-seconds.

6 Evaluating an FHT Application and User Specific Needs

As RT hybrid testing has evolved at the CU NEES FHT Facility a systematic means for evaluating system performance and behavior has been developed and is based on 4 levels of simulation. These levels progressively add sophistication culminating in a RT hybrid simulation. Depending on the nature of a particular hybrid test program the mix of these multiple levels may vary but will provide a valuable means of preparing for the final simulation involving the interaction of numerical and experimental components in realtime. This approach will be illustrated using 2 completed realtime testing programs (1) first, for a simple steal frame structure in which one of the columns is tested well into the nonlinear range and (2) for a MR Damper also tested well into the nonlinear range. A brief general summary of the four progressive levels follows.

6.1 Level 1 Simulation

A series of Level 1 simulations involve a fully numerical or analytical model in which the system response is determined over a range of inputs or stimulus of interest. Typically a finite element model will be used at this initial level. At this stage an existing or perhaps newly developed element will be used in the model to simulate the component that will eventually be tested physically in the laboratory.

Things to consider at this level are

1. Limit as much as is reasonably possible the complexity of the numerical component of the hybrid test structure.
2. Select appropriate ground motion records that are usually in the form of discrete acceleration signals.
3. Construct a model of the experimental component that reasonably approximates the expected response of this component.

4. Develop an understanding of the expected response at the interface between the experimental and numerical components. This information is essential to evaluating the required performance of the testing equipment.
5. Establish a maximum value for the integration time step that will provide stable and accurate results.
6. Select a node and element configuration that captures the important material and structural mechanics of the problem of interest.
7. Establish the damping properties to be modeled in the structure.

Care taken at this preliminary level should simplify and ideally minimize the effort involved in the coming levels of simulation that are progressively more complex.

6.2 Level 2 Simulation

Level 2 simulations begin to focus on the models and algorithms that will be used during the hybrid testing phase. In addition the model must now be clearly divided into the two distinct components, experimental and numerical, that makeup the hybrid structure.

The level 2 simulation begins with the translation of the FEM model into the *tcl* like format that will be referred to as a realtime OpenSees input script. Appendices A and B contain listings of the translated reference model input file. The translation is needed owing to limitations that have prevented the *tcl* interface for OpenSees from being included in the realtime version of OpenSees which currently runs on the PharLap ETS kernel (the realtime OS). A realtime version of the user interface, FHTFrameBuilder, has been developed at CU which parses a model input file and initiates the execution of an analysis. The FHT frame builder has significantly less sophistication than *tcl* as can be seen from a brief study of the input files in Appendices A & B.

For exampe the commands for a transient analysis require modification. Instead of using the command "integrator Newmark" the RT translation is "integrator FHT". This enables the hybrid testing features that are built into the integration method of Hilber, Hughes and Taylor.

The level 2 simulation does not yet contain the experimental substructure but instead has a conventional or newly developed finite element in its place. This level of simulation confirms the proper functioning of the realtime OS, the realtime version of OpenSees as well as all of the derived classes that implement the details of the FHT algorithm.

6.3 Level 3 Simulation

The third level of simulation involves the combined function of multiple realtime computing systems. The Primary host-target which runs the simulation of only the numerical component using OpenSees is now working concurrently with a second RT simulation computer. The second RT system is configured with the RT OS of MathWorks (Realtime Workshop & xPC Target) and is running a RT simulation of the

experimental component including models of the hydraulic actuators. The MTS Digital Controller is setup in simulation mode which disables the signal to the hydraulic actuators but leaves the remaining actuator controls fully operational. The shared memory network (ScramNet) is used to coordinate these three RT computers and pass the time critical control and measurement data between the processors.

This level of simulation utilizes the exact same model at the Primary simulation computer that will be used during the final FHT at level 4. In the final step to level 4 the model of the experimental component and hydraulic actuators is replaced with the actual test hardware.

6.4 Level 4 Simulation

The level 4 simulation now involves the experimental component and its direct involvement in the full hybrid model.

The 3 previous levels of simulations ideally established the needed groundwork to move successfully to the final full hybrid simulation. Trial and error experimentation and other such methods can be done at levels 2 or 3. Levels 2, 3 and 4 should be carried out by the trained staff at the CU NEES FHT facility as significant unique and very specialized software and hardware are involved. The simulations of level 1 can be completed using any computer and at any location.

Depending on the type of testing and equipment involved in any particular hybrid simulation I may be beneficial to alter the details of this multilevel approach. For example if a test involves a device or structural component that has been tested previously, the level 2 and 3 simulations may be simplified or perhaps dropped all together. A decision such as this should be made in close coordination with the staff at CU NEES.

7 FHT on a Steel Frame Hybrid Structure: Accessing System Level Performance Needs & Limitations

The first 3 levels of the four level progressive simulation protocol discussed in Section 4 establishes a systematic means for system and component level evaluation of a hybrid testing plan prior to any physical testing. Level 1 simulations involve a fully numerical or analytical model and make it possible to approximate the simulation demands in terms of actuator performance as well as computational needs. It should also be noted that the CU NEES FHT system is currently limited to a maximum of three DOFs. This can be increased at the expense of adding more hydraulic actuators and controls.

7.1 Preliminary Analysis: Level 1

Lets begin by considering the model developed for the level 1 simulation of a two story two bay steel frame structure where the middle, first story column will be modeled experimentally.   At this initial level of simulation the experimental component is modeled numerically using a force based nonlinear beam-column element.   The remaining portion of the structure is modeled using a combination of linear and nonlinear beam elements. During the level 4 FHT the same modeling components will be used for the numerical portion of the model while the experimental component of the hybrid structure is substituted with the physical component being tested in the lab.

Early in the development of the level 1 model it was recommended that the computational needs for the FEM be evaluated. Two important issues to consider in this area are: 1. What is the largest reasonable value that can be used for the integration time step and still provide an appropriate level of accuracy? 2. Given the established time step and FEM, can the required computations be completed within the allotted time? This second criteria is essential only for realtime testing in which it has been determined that a distortion of testing time is not acceptable.

For example, when the experimental component is subject to rate sensitive behavior realtime will create more realistic testing conditions.   When the response of the experimental component is not rate or velocity sensitive the rate of loading and therefore the time allowed for the computation of each integration step may be arbitrarily varied. Practically speaking some limitations do exist here due to load relaxation effects but in general and historically great liberties have been taking in this area. The CU NEES facility has the ability to accommodate and maintain a consistent time scaling throughout a simulation.   This maintains constant and consistently scaled movement in the experimental component avoiding so called hold periods where the structure remains motionless for indefinite periods of time. For example a 30 second seismic event can be time expanded to take place in 3,000 seconds in the laboratory and a time scaling of 100 is maintained consistently throughout the simulation all the way down to the millisecond level.

7.1.1 FEM Convergence Properties

Figure 2 illustrates the level 1 idealization of the steel structure under present consideration. Table 1 summarizes the element properties in detail. For this structure it is assumed that the nonlinear behavior of the structure will be for the most part limited to the columns and therefore force based nonlinear beam column elements are used for all vertical elements. The remaining horizontal beams will be modeled using linear beam-column elements.   The level 1 model consists of 10 beam elements, 9 nodes and 27 DOFs. A copy of the input file for this model is provided in Appendix A.
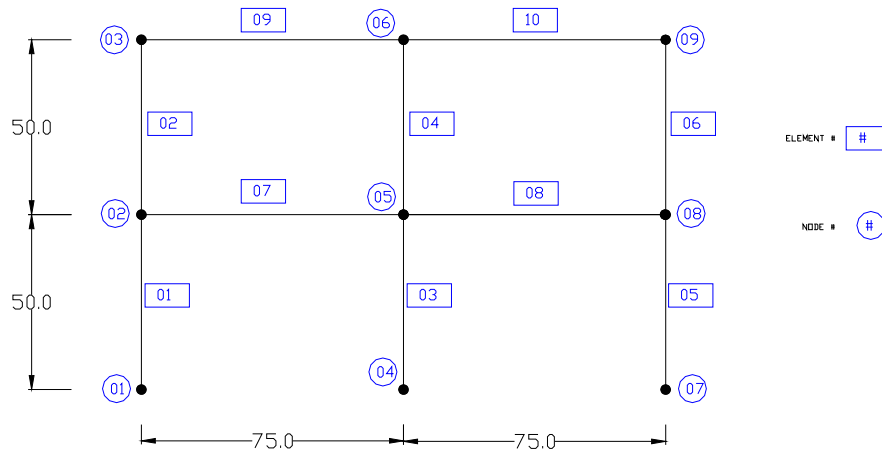
Figure 2: Level 1 Finite Element Model Layout

Scaled copies of the El Centro base motion as recorded on May 18th 1940 in the Imperial Valley of California will be applied to this 2 story 2 bay structure. The x axis (the horizontal direction) of the global structural coordinate system will be oriented in alignment with the major axis of the El Centro motion.

Element #	Element Type	Section Type	E (KSI)	A ($inches^2$)	I ($inches^4$)	F_y (yield strength KSI)	Hardening Ratio (ratio of tangents)
1	Nonlinear Beam-column	W 8x35	29000	10.3	127	55.0	1e-6
2	Nonlinear Beam-column	W 8x35	29000	10.3	127	55.0	1e-6
3	Nonlinear Beam-column	W 8x35	29000	10.3	127	55.0	1e-6
4	Nonlinear Beam-column	W 8x35	29000	10.3	127	55.0	1e-6
5	Nonlinear Beam-column	W 8x35	29000	10.3	127	55.0	1e-6
6	Nonlinear Beam-column	W 8x35	29000	10.3	127	55.0	1e-6
7	Elastic Beam-column	W 14x120	29000	35.3	1380	NA	NA
8	Elastic Beam-column	W 14x120	29000	35.3	1380	NA	NA
9	Elastic Beam-column	W 14x120	29000	35.3	1380	NA	NA
10	Elastic Beam-column	W 14x120	29000	35.3	1380	NA	NA

Table 1: Level 1 FEM Element Properties

The first consideration is the convergence properties for the FEM. That is to say how large of a time step can used during direct time integration of the model and still provide an accurate solution. Figure 3 summarizes a series of level 1simulations with variable integration time steps. The two response curves for $\triangle t=0.01$ and 0.001 are very nearly identical while the remaining curves show a large variation in the response. Based on these results we can establish the integration time step of 0.01 seconds as a reasonable value and will use this value for all subsequent simulations, levels 1-4.
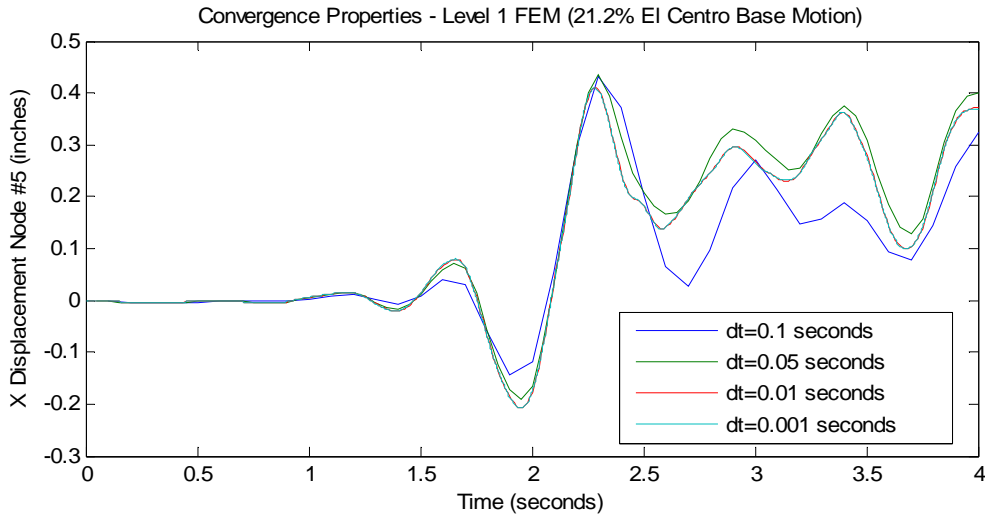
Figure 3: Level 1 Finite Element Model

With the integration time step established it must be determined that the model, nonlinear in this and probably most cases, can be solved in a timely manner avoiding timing conflicts and the resulting distortion of testing time. Here it is assumed that it has been determined that realtime hvbrid simulations are needed. If they are not then the following discussion is not relevant and the simulations could be carried out in scaled or expanded time.

7.1.2 FEM Complexity and Size Considerations

It is not uncommon for a FEM (node, element and material configuration) to be constructed in a more elaborate and complex form than is absolutely necessary. For RT hybrid simulations this has the potential of creating a problem by making it difficult to run the simulation with sufficient speed for RT testing. In general it is important that the model size and complexity be limited such that 10 iterations of the nonlinear Newton-Raphson solution procedure are completed within the allotted time for each integration time step, 0.01 seconds. Determining this is clearly dependant on the computer used as well as other hardware and software involved in a simulation. The CU NEES FHT laboratory is supported with annual operation and maintenance funds provided by NEES

Inc. A portion of these funds are budgeted so as to keep the primary FHT computation computer up to date with the latest software and hardware.

The CU FHT system utilizes a realtime operating system which adds a high degree of determinacy and repeatability to the solution process. Ideally a prospective user should work directly with the staff at CU NEES to establish some reasonable bounds for the level of sophistication for the model. The model used here for the 2 story 2 bay steel structure easily runs in RT.

7.1.3 Level 1 FEM Response Considerations

The response of node number 5 during level 1 simulation can be used to determine the expected performance requirements of the hydraulic test equipment in terms of peak displacements, velocities and forces. Figure 4 illustrates how the three hydraulic actuators are configured to allow for control of the three model DOFs at node 5 (horizontal, vertical and rotational displacements).
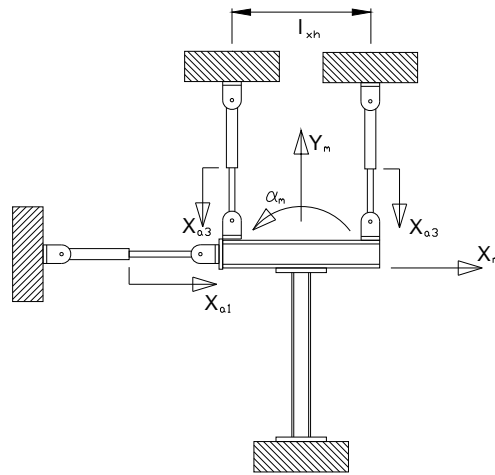
Figure 4: Three Actuator Configuration: Experimental Component

The 3 degrees of freedom may be expressed either in model or actuator coordinates. The actuator coordinates are all linear displacements with extension defined as positive and actuator compression also defined as positive force. The level 1 simulation results, shown in Figure 5, are the output of the FEM and as such are in terms of model coordinates. These are response curves for node 5 when the structure is subject to 21.2% of the full scale El Centro uniform base motion. It should be noted that some of the results presented throughout this level 1 discussion will include response data from level 4 FHTs and are presented primarily for comparison purposes. Similarly, during the level 4 discussion some of the results from level 1 simulations will be presented.
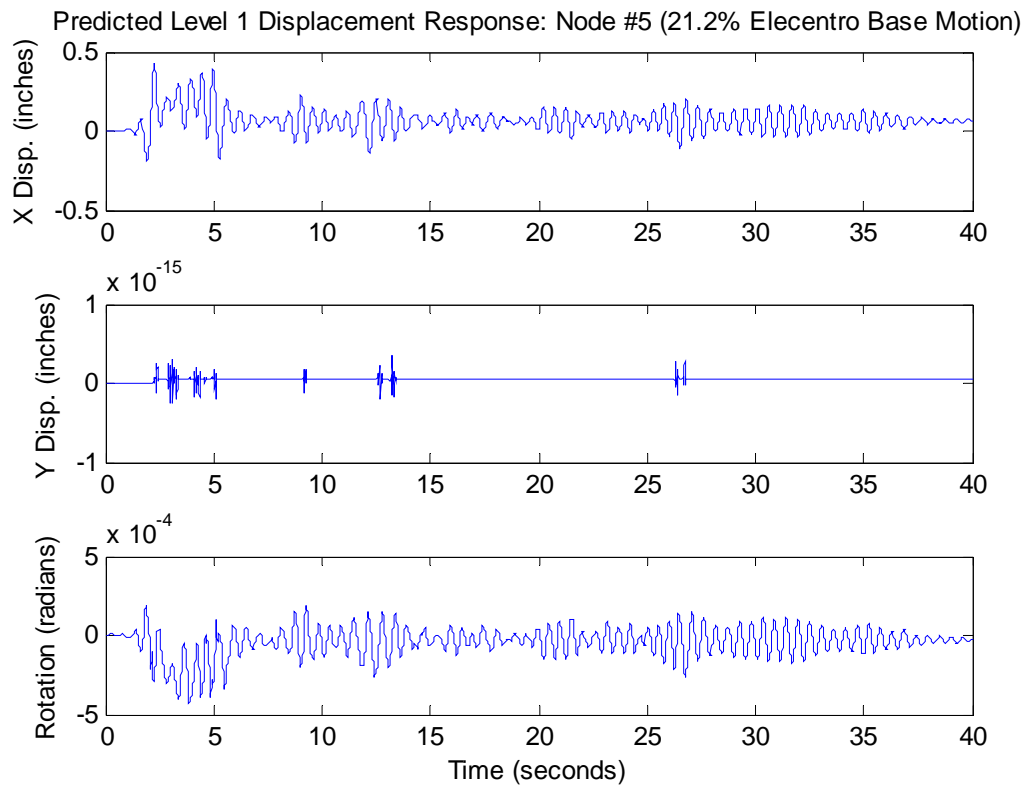
Figure 5: Predicted Displacement Response Histories
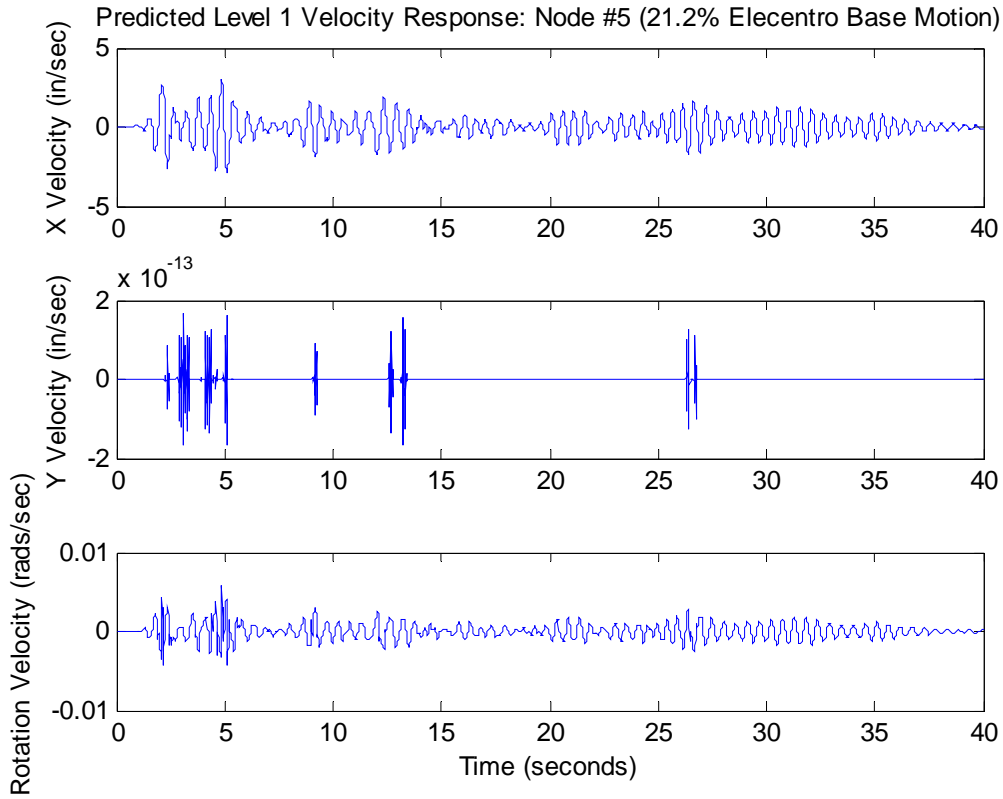
Figure 6: Predicted Velocity Response Histories (in model coordinates)

In order to evaluate the required performance of the actuators and testing system these displacement and velocity results must be transformed to actuator coordinates. The transformations from model to actuator displacements and model to actuator forces are derived from the kinematics, illustrated in Figure 4, and are

$$T_1 x_m = x_a \qquad\qquad \textbf{Equation 1}$$

$$T_2 f_m = f_a \qquad\qquad \textbf{Equation 2}$$

where

$$T_1 = \begin{bmatrix} 1 & 0 & 0 \\ 0 & -1 & \dfrac{l_{xh}}{2} \\ 0 & -1 & \dfrac{-l_{xh}}{2} \end{bmatrix}, \quad x_m = \begin{Bmatrix} x_m \\ y_m \\ \alpha_m \end{Bmatrix}, \quad x_a = \begin{Bmatrix} X_{a1} \\ X_{a2} \\ X_{a3} \end{Bmatrix} \qquad \textbf{Equation 3}$$

$$T_2 = \begin{bmatrix} 1 & 0 & 0 \\ 0 & -0.5 & \dfrac{2}{l_{xh}} \\ 0 & -0.5 & \dfrac{-2}{l_{xh}} \end{bmatrix}, \quad x_m = \begin{Bmatrix} x_m \\ y_m \\ \alpha_m \end{Bmatrix}, \quad x_a = \begin{Bmatrix} X_{a1} \\ X_{a2} \\ X_{a3} \end{Bmatrix}. \qquad \textbf{Equation 4}$$

Where the subscripts *m* and *a* are used to indicate model and actuator coordinates respectively. The response curves shown in Figure 7 and Figure 8 are in terms of the actuator degrees of freedom and may be used in comparison to the MTS actuator performance curves shown in Appendix C.
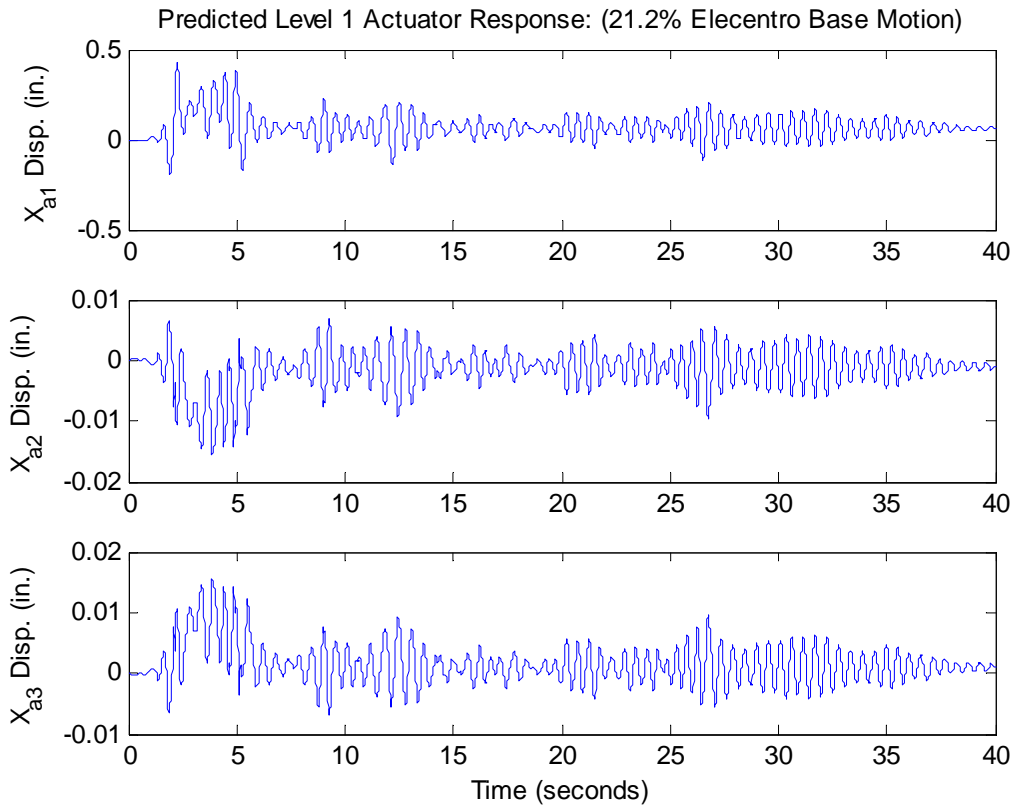
Figure 7: Predicted Displacement Response Histories (in actuator coordinates)

The peak displacement values are well within the stroke capacity for each of the respective actuators. Additionally, the peak velocities taken from Figure 8 are also well within the velocity capacity.

24
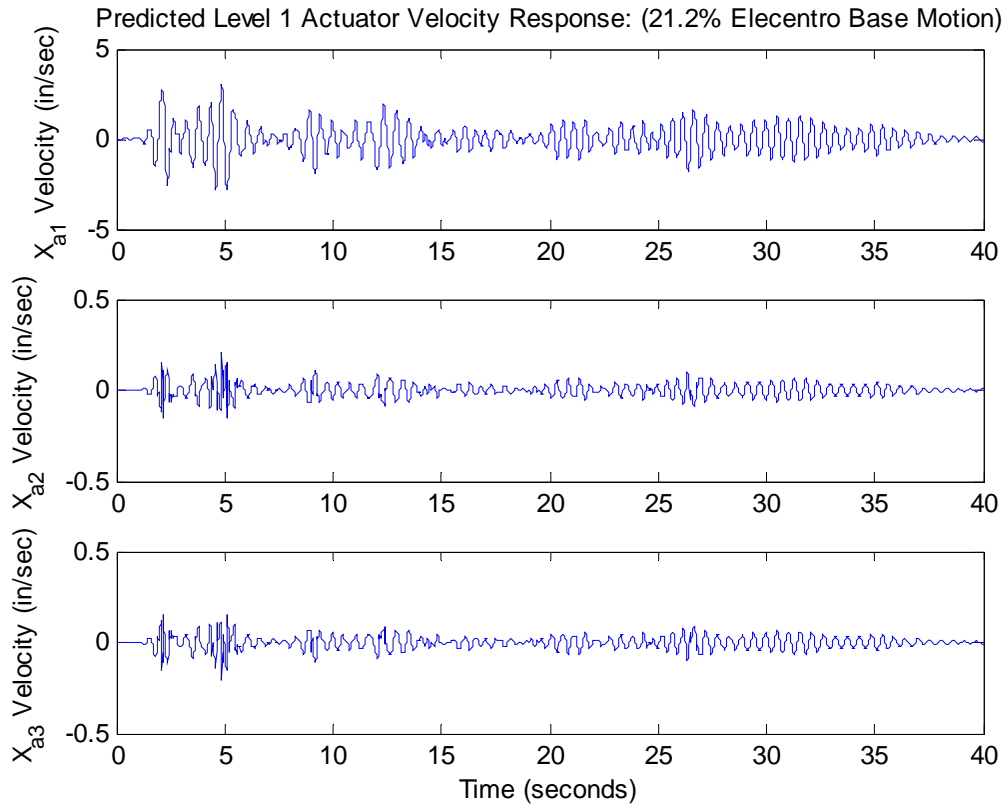
Figure 8: Predicted Velocity Response Histories (in actuator coordinates)

In addition to displacement and velocity considerations force must also be evaluated. Approximate predictions for actuator force histories can be obtained using the linear stiffness matrix for the column being tested. In this case the inertial portion of the applied external force may be neglected due to the small mass and low accelerations associated with this experimental test component. Predicted and measured forces for this case are shown in Figure 9.
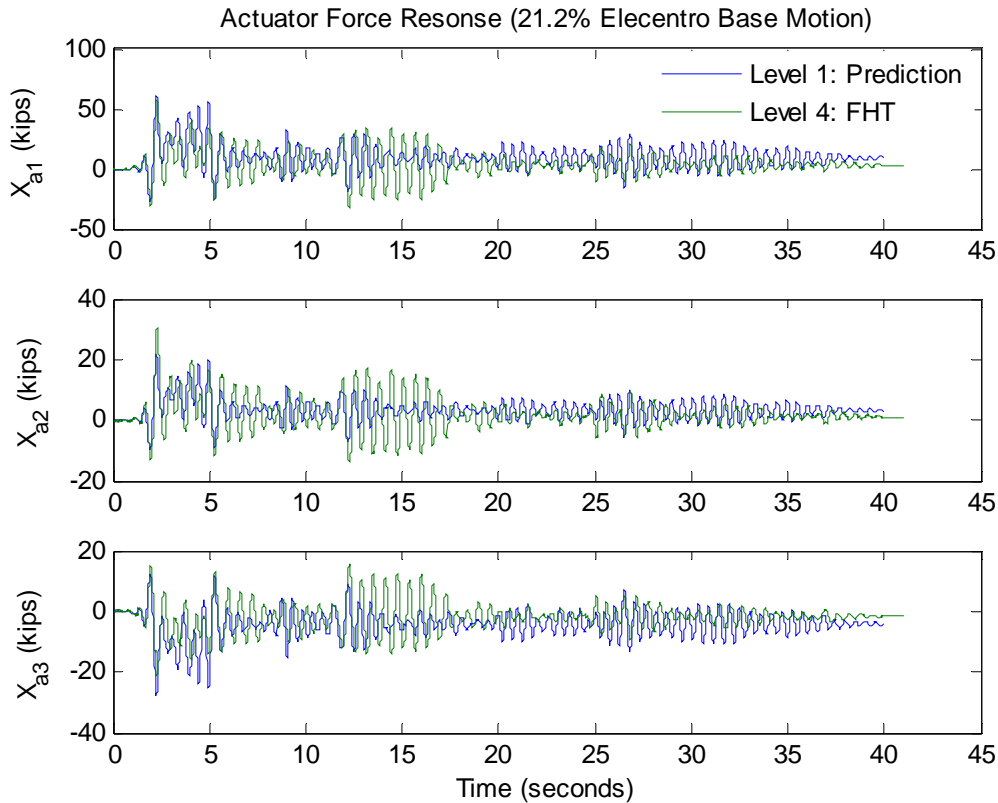
Figure 9: Predicted & Measured Actuator Force Histories

The actuator force predictions in this case serve to confirm that for this test the actuator force capacities will not be exceeded throughout the simulation. The force measured during the actual FHT is also shown and appears to compare favorably in general. Certainly for the purposes of establishing approximate anticipated forces prior to testing this method works adequately well, as it should, due to the very limited nonlinear behavior for this low level of base excitation. As the base excitation is increased and the experimental component is pushed well into the nonlinear range we can expect the quality of such a prediction to be reduced.

7.2 Level 2 and 3 Simulations

For the simple structure, under consideration here, simulations at levels 2 and 3 are used primarily to confirm the correct operation of the FHT system including the realtime shared memory network. These simulations were being carried out during this final phase of the equipment procurement and development phase of the CU NEES FHT facility. The formalization of the 4 level simulation sequence was not yet in place and simulations for the intermediate levels (2 and 3) were conducted but not made a part of the permanent data archive.

7.3 Level 4: Realtime FHT with Strong Nonlinear Restoring Force Behavior

The final level of simulation involves the full hybrid structure engaging concurrently both the experimental and the numerical portions of the model in realtime. While we consider this level of simulation we will work with the response and prediction data from the final and strongest base motion (78% of El Centro). The level 1 simulation, involving a purely numerical FEM, will be shown for comparison purposes.

This final test on the W 8x35 column involves strong nonlinear behavior which is most evident in the restoring force term of the experimental component. The level 1 through 3 simulations were carried out as described and have thus provided bounds for the expected peak displacements, velocities and forces. These results are summarized below in Figure 10 thru Figure 12.
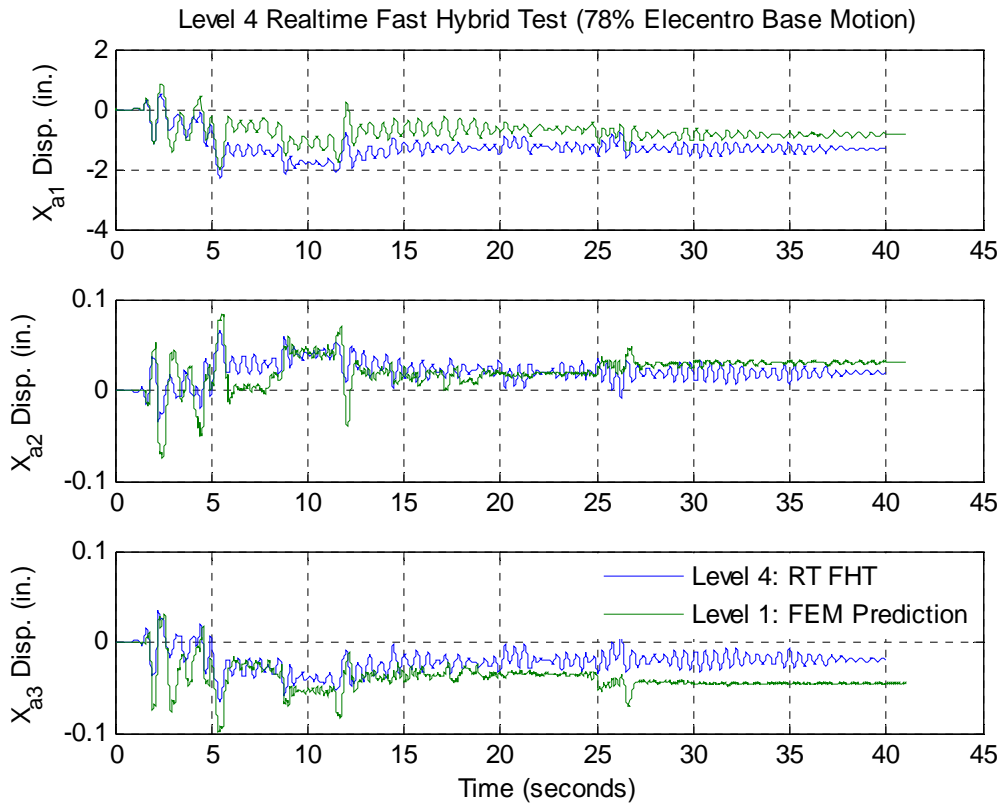
Figure 10: Level 4 Actuator Displacement Response Histories

The level 1 prediction for this, the most severe of the tests, is also shown in Figure 10 and provides a pre-FHT indicator that the actuators remain within there respective displacement performance envelopes. With regard to the velocity predictions shown in Figure 11, the capacity of the large 220 kips actuator is very near its 10 inches/second

limit. During this test there was no direct measurement of velocity but a comparison of the displacement command and response signals at the time of highest velocity can provide a very good indicator of the system performance. Figure 12 shows the very accurate tracking that occurred during this high velocity period of the test, indicating that the large actuator is successfully achieving its velocity capacity.
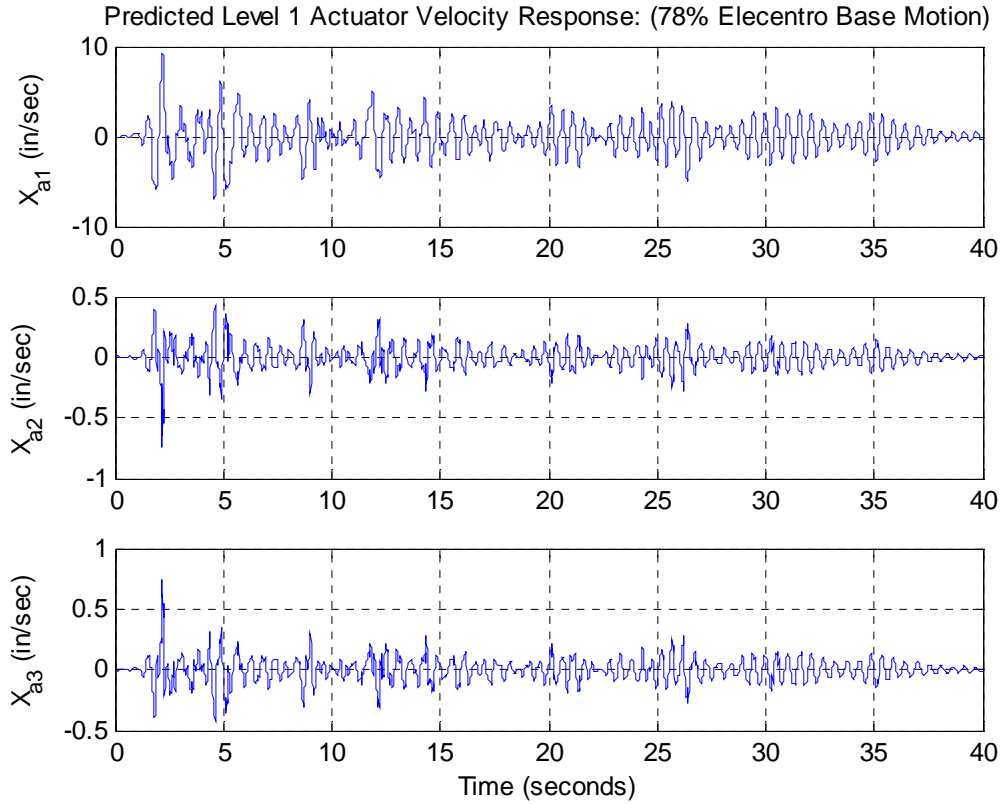
Figure 11: Level 1 Predicted Actuator Velocity Response Histories
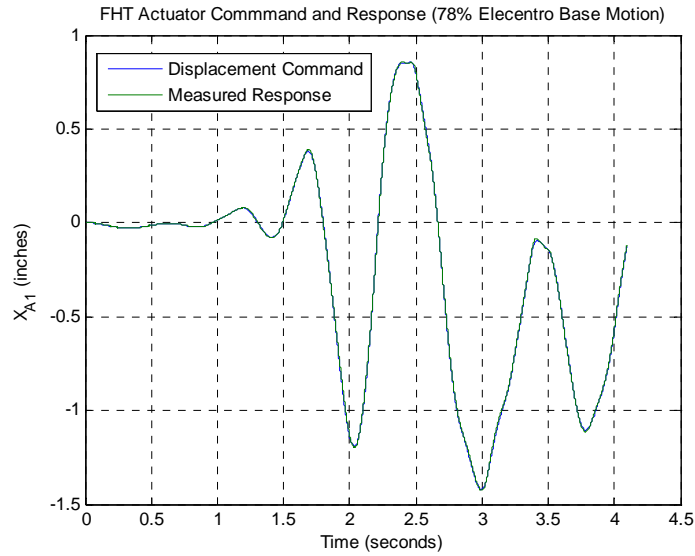
Figure 12: Actuator 1 Response Near Velocity Limit

The actuator force histories are summarized in Figure 13 and for comparison purposes the predicted forces obtained during the level 1 simulation are also shown. The level 1 prediction in this case is reasonably accurate largely due to the nonlinear forced based beam-column element used to model this component. It is likely that in other testing scenarios such an accurate model may not be available and sound reasoning and judgment will need to be used to construct a model that will provide reasonable level 1 results.
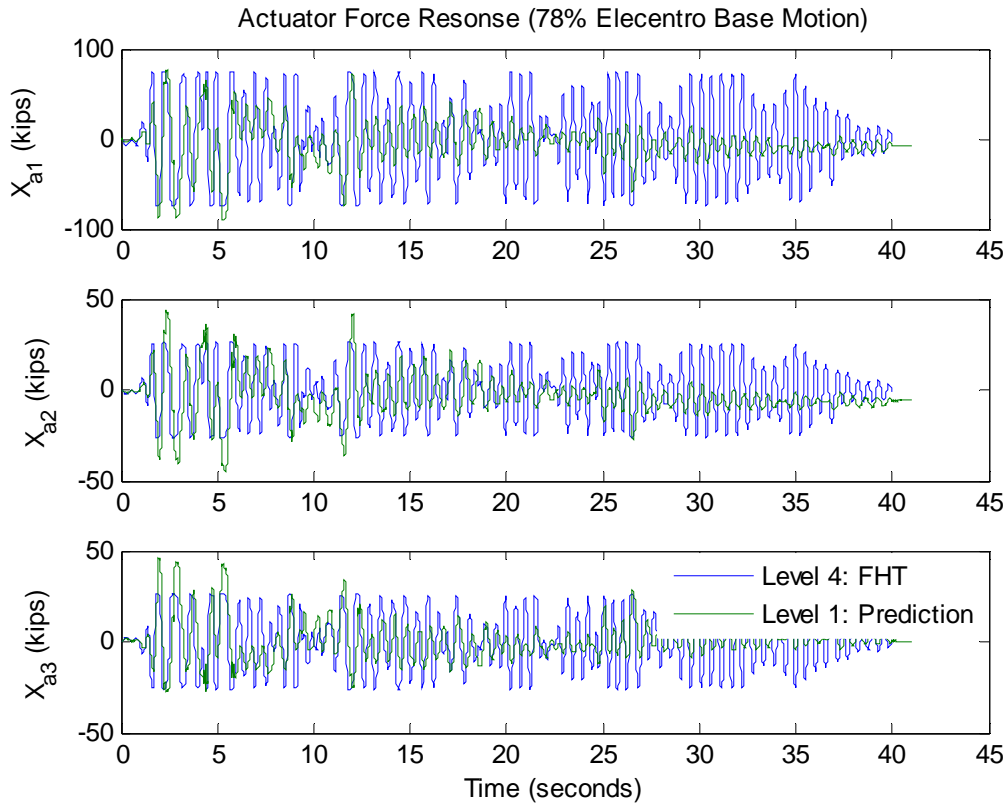
Figure 13: Actuator Force Response Histories

The presence of substantial nonlinear behavior is clearly seen in Figure 14 showing the significant and repeated excursions into inelastic behavior. The vibrations which can be seen near some of the force peaks is likely a result of the slipping of the column-support interface. Somewhat surprisingly this additional source of nonlinear behavior did not cause any difficulties for the integration process. This additional source of energy dissipation may explain the difference between the predicted and measured force response histories shown in Figure 13.
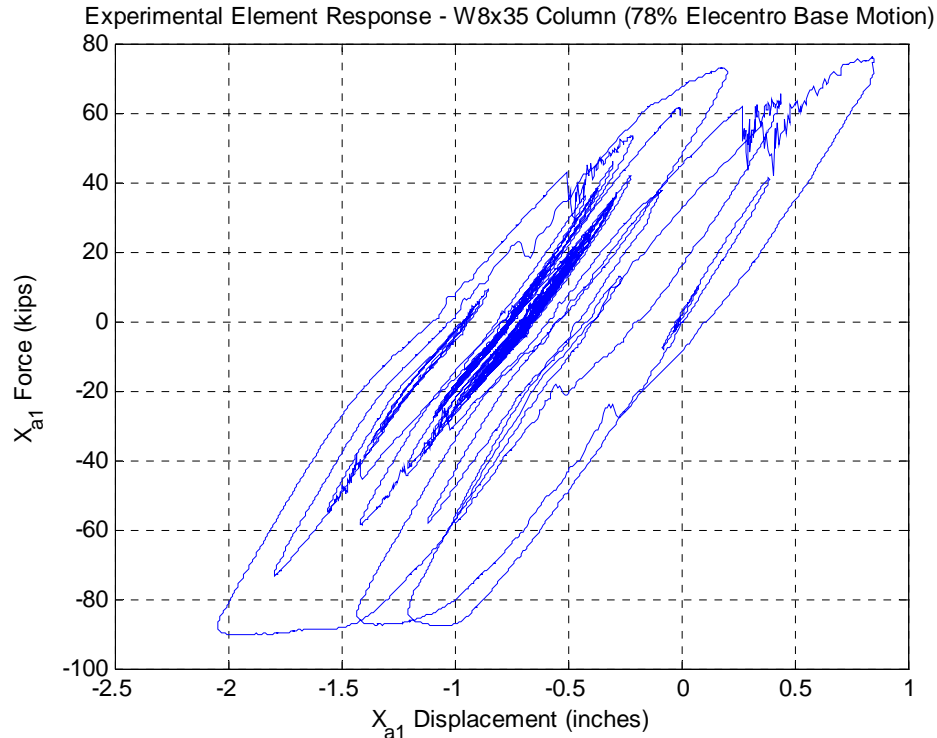
Figure 14: Level 4 Actuator Force vs Displacement

It is noted that all of these tests were completed in hard real time with not a single violation of the timing constraints within the direct time integration scheme.

8 FHT with a Nonlinear Damping Device: Accessing System Level Performance Needs & Limitations

The Magneto-Rheological (MR) damper has been the subject of considerable research in recent years with interest in using it as a passive or so called semi-active device for earthquake damage mitigation. During the summer of 2007 CU NEES FHT facility and Prof. Christenson concluded an investigation of these devices under a variety different testing and control conditions. CU NEES was entrusted with one of those dampers and it was used to independently perform the next series of validation tests.

The MR damper will be the focus of a series of benchmark hybrid tests presented here and intended to highlight the capabilities and limitations of the CU NEES FHT system. These benchmark tests will explore the current capabilities (as of Fall 2007) for the CU FHT system in the following areas. Series 1 will establish FHT accuracy as well as model size limitations working primarily in the linear range of the numerical and experimental test components. Series 2 benchmark tests systematically extend the results from the linear range into nonlinear behavior. The third series of tests focuses on actuator related performance issues and there effects on hybrid simulation results. The

fourth series investigates the significance of hard realtime as opposed to soft realtime. Where the term soft realtime is used here to indicate a variety of differing deficiencies in the correct and accurate replication of simulation time. It is perhaps worth mentioning that some of these so called soft realtime simulations are what many others in the hybrid testing community have been loosely referring to as realtime.

A brief summary is provided of the new generalized implicit integration technique used in the following tests. This generalization is motivated by the understanding that existing hybrid testing algorithms proceed on the assumption that the test component is a structural element. In other words the test component responds to an applied displacement with a corresponding force. The force output of the MR damper is more accurately represented as a highly nonlinear velocity dependant device in which the test component responds to an applied velocity with a corresponding force. This distinction is in fact what necessitates that a damping device must be tested under hard realtime conditions.

8.1 Generalized Implicit Hybrid Testing Algorithm

Most hybrid testing techniques are based on the application of direct time integration techniques to a discrete representation of the governing equations of motion. The discrete representation consists of both numerical and experimental components which together constitute a hybrid model of a structure. The direct time integration approach used here extends the implicit integration technique developed by Shing et al[2] to allow for a nonlinear damping element. This method begins with the α – method established by Hilber et al.[3] and Hughes[4] and applies several constraints in order to achieve the conditions need for realtime hybrid testing. A dynamic structural system may be expressed as

$$Ma + s(v) + r(x) = f.$$ **Equation 5**

In which M is the system's discrete mass matrix and s, r and f are vectors representing the nodal damping, restoring and external forces respectively. The quantities a, v and x are the nodal acceleration, velocity and displacement vectors. It is noted that both the damping and the restoring force components allow for a nonlinear relationships between there respective dependant and independent variables. The parameters α, β and γ are now plugged in the equation of motion in agreement with Hilber and Hughes

$$Ma_{n+1} + (1+\alpha)s_{n+1} - \alpha s_n + (1+\alpha)r_{n+1} - \alpha r_n = (1+\alpha)f_{n+1} - \alpha f_n$$ **Equation 6**

$$d_{n+1} = d_n + \Delta t v_n + \Delta t^2 \left[(1/2 - \beta)a_n + \beta a_{n+1}\right]$$ **Equation 7**

$$v_{n+1} = v_n + \Delta t \left[(1-\gamma)a_n + \gamma a_{n+1}\right].$$ **Equation 8**

Where the subscripts n and $n+1$ are introduced to indicate the discrete and successive values of a variable at a given instant in time where $\Delta t = t_{n+1} - t_n$. In the linear case unconditional stability can be obtained with $\beta = (1-\alpha)^2/4$, $\gamma = 1/2 - \alpha$ and $-1/3 \leq \alpha \leq 0$.

This direct method of time integration enforces equilibrium at evenly spaced time intervals which herein will be referred to as the *integration interval*. In order to allow for nonlinear structural response it is necessary to include an iteration capability that converges to the equilibrium condition within each integration interval. A modified Newton-Raphson iteration method is used. For realtime simulations the number of iterations will be constrained to a fixed and constant number[5] which effectively subdivides the integration interval into l *iteration intervals*. If each of these l subintervals is further constrained such that all subintervals are equal in time we have

$$\delta t = \frac{\Delta t}{l}.$$
Equation 9

Where Δt and δt are the time intervals associated with the integration and iteration intervals respectively. By fixing l to be a constant integer value the iteration process is made more deterministic which proves to be helpful for realtime integration and hybrid testing. This determinism comes at the price of constraining the calculation of equilibrium to a limited number of Newton iterations that each must be completed in a fixed interval of time. Experience at the CU NEES FHT facility has shown 10 to be a reasonable selection for l and 0.01 seconds for Δt.

A simplified discrete representation of the force equilibrium equation in residual form is obtained by solving Equation 7 for a_{n+1} and substituting into Equation 6

$$f_v = M d_{n+1} + c_0 + c_1(s_{n+1} + r_{n+1}) = 0.$$
Equation 10

Where

$$c_0 = -M[d_n + \Delta t v_n + \Delta t^2 (\frac{1}{2} - \beta)a_n] - \Delta t^2 \beta [\alpha(s_n + r_n - f_n) + (1+\alpha)f_{n+1}]$$
Equation 11

$$c_1 = \Delta t^2 \beta (1+\alpha)$$
Equation 12

Equation 10 contains two unknowns, v_{n+1} and d_{n+1}, which are independent variables for the damping and stiffness terms respectively that have both been treated as general nonlinear relationships. By combining equations 7 and 8 an equation expressing v_{n+1} in terms of known quantities and d_{n+1} is obtained

$$v_{n+1} = \frac{\gamma}{\beta} \left[\frac{1}{\Delta t}(d_{n+1} - d_n) + (\frac{\beta}{\gamma} - 1)v_n + \Delta t(\frac{\beta}{\gamma} - \frac{1}{2})a_n \right].$$
Equation 13

With equations 13 and 10 a general modified Newton iteration procedure can be used to solve for the unknown discrete displacement field d_{n+1}. The iterative solution procedure is based on the linearized representation of the residual equilibrium equation

$$f_r(d_{n+1} + \Delta d) \approx f_r(d_{n+1}) + \frac{\partial f_r}{\partial d_{n+1}} \Delta d. \qquad \textbf{Equation 14}$$

Where successive displacements increments Δd are computed until a convergence criterion is satisfied indicating equilibrium has been achieved. The Jacobian in Equation 14 may be expressed as

$$\frac{\partial f_r}{\partial d_{n+1}} = M + c_1 \left(\frac{\partial s_{n+1}}{\partial v_{n+1}} \frac{\partial v_{n+1}}{\partial d_{n+1}} + \frac{\partial r_{n+1}}{\partial d_{n+1}} \right). \qquad \textbf{Equation 15}$$

With some manipulations and approximating the tangent stiffness and tangent damping matrices in Equation 15 with the initial stiffness and damping matrices, K_i and C_i the displacement at the kth Newton iteration may be calculated using

$$d_{n+1}^{k+1} = d_{n+1}^k - \frac{f_r(d_{n+1}^k)}{M + c_1 \left(\dfrac{\gamma}{\Delta t \beta} C_i + K_i \right)} \qquad \textbf{Equation 16}$$

In considering the use of Equation 16 in a realtime hybrid testing scheme it becomes clear that the displacement value(s) that correspond to the node(s) of the experimental component need to be treated separately from the remaining nodal displacement values. Recall that Equation 9 implies that there will be l, consistently spaced in time, computations involving the solution of Equation 16. The computation of the force residual in the numerator is carried out using the previous displacement solution d_{n+1}^k which implies that forces measured from the experimental component must be taken with the actuator at this position (also in essence implying that the actuator velocity must be v_{n+1}^k). If this was possible and were to be the case it would lead to a very rough tracing of the equilibrium path during the Newton iterations, this is not a problem for the FEM portion of the structure but certainly is for the experimental component. This problem is overcome be using a best fit quadratic polynomial to interpolate and generate the actuator command signal(s). The two prior converged or committed solutions (x_{n-1}, x_n) are used along with the most recently calculated value of the next solution (x_{n+1}^k) to determine the quadratic polynomial coefficients.

Figure 15 illustrates the interpolation process for the simplified case of $l = 3$. For hard realtime testing the simulation time associated with the direct time integration and the testing time are for all practical purposes one and the same. The blue points indicate the point in time when the solution becomes available (although this solution point corresponds to the point in time at the end of the current integration interval). So at these intermediate points in time when $t = t_n + k \cdot \delta t$ the interpolated points shown in red are computed using a best fit quadratic polynomial for the triplet $(x_{n-1}, x_n, x_{n+1}^k)$. In this way

an actuator command sequence is generated which is smooth and a more accurate approximation of the true equilibrium path.
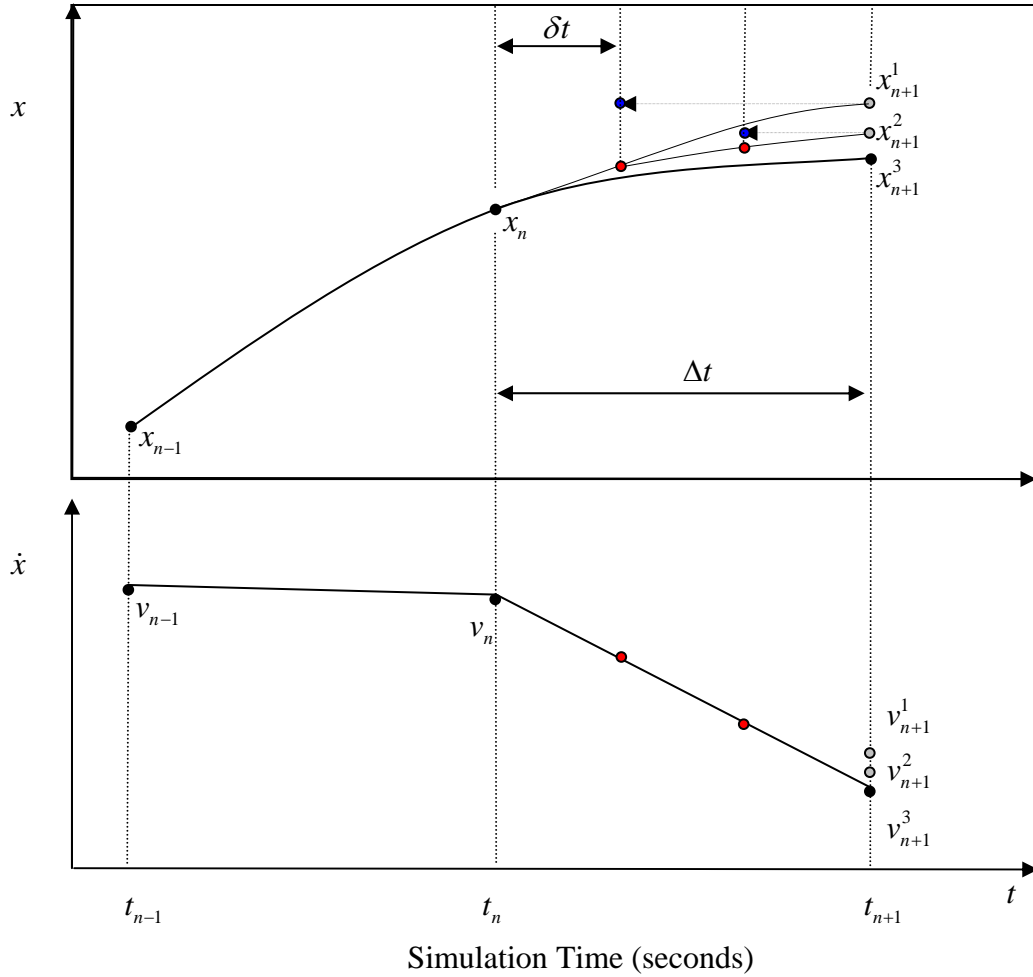
Figure 15: Displacement Command Interpolation

Figure 15 also illustrates how there is now an inconsistency in that the force must be measured from the experimental component at the interpolated points while equilibrium is being determined at the end of the current integration interval. Ideally the measured force at each iteration would be taken from the experimental component at the position and velocity of the kth solution. To compensate for this a correction needs be applied to each force measurement that is taken along the interpolated path between x_n and x_{n+1} using

$$f_{n+1}^k = f_{n+1}^{M(k)} + K_i(x_{n+1}^k - x_{n+1}^{M(k)}) + C_i(v_{n+1}^k - v_{n+1}^{M(k)}).$$ **Equation 17**

The super script, $M(k)$, is used to indicate values that are measured from the experimental test component. In addition to compensating for the force discrepancy, arising from the actuator command interpolation, this also compensates for imperfection, be it phase lag or lead in the actuator command-response. Using this approach it is possible and in most cases likely preferable to interpolate only the nodes associated with the experimental component and apply this force correction to only the measured forces taken from the experimental component. Ideally both the initial stiffness and initial damping matrices in Equations 16 and 17 would be replaced with respective secant or tangent matrices but this level of sophistication is yet to be successfully developed, tested and implemented. Indeed, currently only the displacement portion of the correction is in use. In order to properly implement the velocity term there is the as of yet unmet need for an accurate and reliable velocity measurement. It would be possible to apply the velocity correction without such a transducer by simply assuming that the measured velocity $v_{n+1}^{M(k)}$ is the current interpolated velocity $v_{n+1}^{I(k)}$. This approach would compensate for the command interpolation but ignore actuator performance inaccuracies.

Another alternative is to attack this problem from a control perspective and through the use of advanced control algorithms eliminate any actuator delay. This approach certainly has its merits but would not resolve the discrepancy in the force measurement that is a result of the command interpolation process. Ultimately some reasonable and effective combination of advanced control techniques and algorithm based force correction such as Equation 17 seems most appropriate.

The fixed number of Newton iterations described above has the potential to introduce errors resulting from cutting short a highly nonlinear problem. Presently this is dealt with by a post-processing capability that allows for the retention and analysis of the norm of the equilibrium residual. The demands of realtime testing limit the extent of modifications, i.e. branch switching or algorithm switching that may be done on the computational fly.

8.2 Benchmark Structures

Two relatively simple structures will be used repeatedly throughout this report: 1) a single column structure and 2) a two story two bay frame structure. The single column test structure consists of a 52 inch long steel W14x257 column which is fully fixed at its base. A concentrated mass is added to the top of the column which is damped at 6.7 percent of critical damping using Rayliegh damping. The MR damper is then added as a horizontal element connected at the top of the column providing considerable additional damping. The single column structure is illustrated in Figure 16 and the convention of using blue to indicate the numerical and red the experimental portions of the hybrid structure is used.
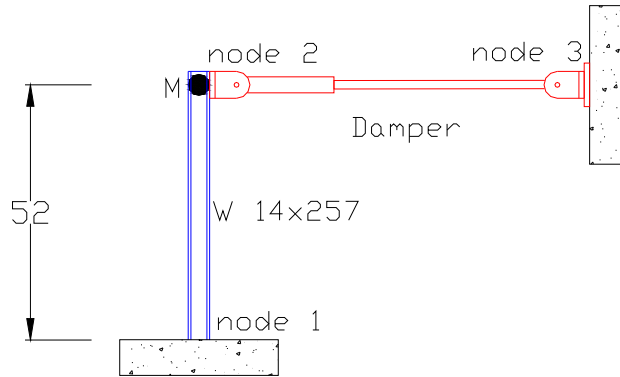
Figure 16: Model Configuration for Single Column Structure

A linear model is created using a conventional two dimensional structural element. Also a nonlinear model is created using the Fiber based nonlinear beam column element[6]. The Eigen values for this structure are summarized in Table 2 below.

Single Column Eigen Values	
Mode #	ω natural frequency
1	18.85 (3.0 Hz.)
2	205.3 (32.7 Hz.)
3	2.754e5 (43,832 Hz.)

Table 2: Natural Frequencies for Single Column

The two story two bay steel frame structure also consists of 2 dimensional structural elements arranged as shown in Figure 17 with the lone experimental component (an MR damper) positioned diagonally within the right hand side first story bay. The linear model utilizes standard 6 DOF linear elastic beam elements only. For the nonlinear model all of the columns are based on the same nonlinear beam-column element used for the single column structure while all of the beams are based on the beam-with-hinges element[7].
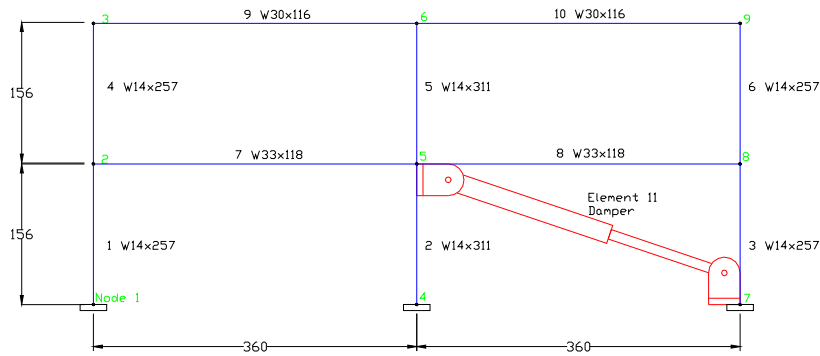
Figure 17: Element and Node Configuration 2 Story 2 Bay Structure

The first five eigen values for the 2 story 2 bay frame structure are shown in Table 3 below.

2 Story 2 Bay Structure Eigen Values	
Mode #	ω natural frequency
1	11.31 (1.80 Hz.)
2	37.43 (5.96 Hz.)
3	86.77 (13.8 Hz.)
4	95.17 (15.1 Hz.)
5	101.1 (16.1 Hz)

Table 3: Natural Frequenies for 2 Story 2 Bay Structure

The complete details for both of the single column and 2 story 2 bay structures can be found in Appendix A: OpenSees Input Files .

8.3 MR Damper Laboratory Setup & Visco-Truss Element

The configuration of the MR damper used in all of these benchmark tests is shown in Figure 18. The damper (seen to the right in the foreground) is oriented horizontally in the CU NEES hybrid testing laboratory with a single 110 kip MTS hydraulics actuator (seen to the left in the background) precisely aligned with the motion of the damper piston. A constant 2.5 Amp current is supplied to the damper for all benchmarks.

Figure 18: MR Damper Laboratory Setup

For comparison purposes and all of the level 1 (fully numerical) simulations a visco-truss element has been added to OpenSees to act in place of the MR damper. In the simulations that involve this element it is oriented exactly as the damper. This element is constructed using standard 2 dimensional truss elements and the viscous material class. The visco-truss element behaves as ideal linear viscous damper that has a constant damping coefficient of approximately 45 Kips/in./second. Below in Figure 20 a direct comparison of the visco-truss element and the output of the MR damper are shown.

8.4 Damper System Identification Tests

The characteristics identified by a series of 15 system ID tests will prove to be useful for the damper benchmark tests and are briefly summarized here. Prior system ID testing carried out by Prof. Christenson did not restrict the velocity magnitude sufficiently to limit the MR damper response to what we will loosely call the linear force-velocity range. All of these additional ID tests do this and explore a limited range of frequencies and velocity amplitudes. During each of the tests the excitation is limited to a single frequency while accurate force, displacement and actuator command signals are digitally recorded at 1024 Hz. using the NI DAQ system.

These system ID tests are motivated by the need to conduct a series of realtime hybrid simulations in which the damper, as much as possible, behaves as a linear viscous damping device. This will make it possible to compare FHT results directly to highly accurate numerical or analytical results. These comparisons serve as a basis for verifying the correct functioning of the hybrid testing algorithm and technology applied at the CU NEES hybrid testing facility. A summary of the ID test is provided in Table 4.

ID Test #	Frequency (hz.)	ω (rads/sec)	D_0 (inches)	V_0 (in/sec)	C_i (in/sec)
1	1.00	6.2852	0.0477	0.30	44.4
2	1.00	6.2852	0.0398	0.25	44.3
3	1.00	6.2852	0.0318	0.20	43.7
4	1.00	6.2852	0.0239	0.15	43.3
5	1.00	6.2852	0.0159	0.10	42.1
6	0.50	3.1426	0.0955	0.30	60.9
7	0.50	3.1426	0.0796	0.25	56.8
8	0.50	3.1426	0.0636	0.20	55.8
9	0.50	3.1426	0.0477	0.15	56.1
10	0.50	3.1426	0.0318	0.10	58.3
11	0.10	0.6285	0.4773	0.30	63.6
12	0.10	0.6285	0.3978	0.25	67.0
13	0.10	0.6285	0.3182	0.20	65.0
14	0.10	0.6285	0.2387	0.15	64.9
15	0.10	0.6285	0.1591	0.10	70.4

Table 4: System ID Testing Matrix and Results

As Table 4 indicates each of these tests involve the application a specified single frequency displacement input to the MR damper.

$$d(t) = D_0 \sin(\omega t)$$ **Equation 18**

By limiting the velocity $(V_0 = D_0 \omega)$ to no more than 0.3 inches/second the damper is nearly behaving as a linear viscous damper. The last column shows the results of a linear curve fit to the force-velocity data set. This value will be designated the initial viscous damping coefficient, C_i. In Figure 19 the deviation from a perfectly linear viscous damper is seen graphically as the differing paths taken as the velocity increase positively as opposed to negatively. Some what surprisingly as the excitation frequency is slowed down these two paths begin to converge.
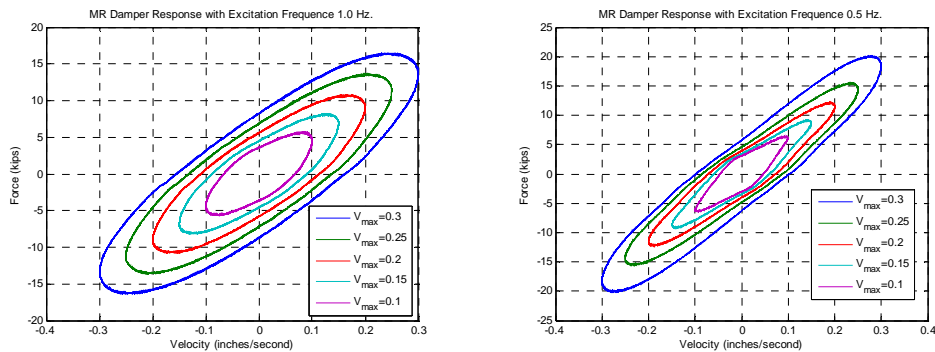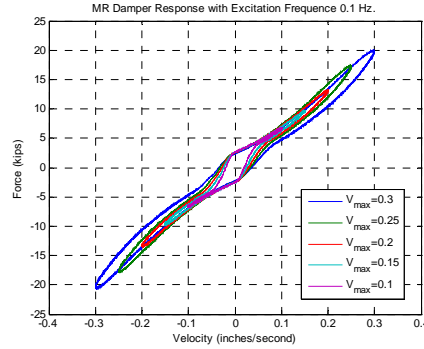
Figure 19: System ID Force vs. Velocity Response Data

In order to arrive at a single C_i value that can be used for a given frequency the average value is taken from the 5 values obtained at differing maximum velocities. These average values are tabulated below.

Excitation Frequency (hz.)	Mean C_i value (in/sec)
1	43.6
0.5	57.6
0.1	66.2

Table 5: Average Initial Damping Values for MR Damper

8.5 A Simple Linear Damper Model

Phenomenological models of the MR damper have been presented by many researchers among them Spencer et. al.[8] and Gavin[9]. By restricting the maximum velocity of the input motion the complex nonlinear behavior of the MR damper is avoided and the simplified model presented here provides good accuracy. The force vs. velocity curves generated by the system ID tests shown previously have a distinctly elliptic shape, especially for the excitation frequencies of $\omega = 2\pi$ and π. A simple linear two term model can be used to accurately represent this behavior.

$$f_d = c_d \dot{x} + k_d x \qquad \textbf{Equation 19}$$

where the parameters c_d and k_d are selected to provide a response that matches the system ID data. The motion for the system ID tests is harmonic which implies that Equation 19 may be rewritten as

41

$$f_d = b_1 \cos(\omega t) + b_2 \sin(\omega t)$$

Equation 20

where

$$b_1 = c_d x_0 \omega$$

Equation 21

$$b_2 = k_d x_0.$$

Equation 22

The values of x_0 and ω are the displacement amplitude and frequency of excitation. A summary of the values used to generate subsequent pure simulation results involving the visco-truss damper model are provided in Table 6 below.

Linear Damper Model Parameters						
	x_0	v_0	b_1	b_2	c_d	k_d
$\omega = 2\pi$	0.0477	0.30	14.0	9.0	46.7	188.7
$\omega = \pi$	0.0955	0.30	6.7	18.7	62.33	65.97
$\omega = 0.2\pi$	0.4773	0.30	20.4	2,5	67.9	5.24

Table 6: Damper Model Parameters Based on System ID Results

Figure 20 shows a comparison of the results obtained from the two parameter damper model and the data collected during the system ID testing. At this frequency the model clearly provides a good match of the measured response.

8.6 Series 1: <u>Accuracy</u> and Model Size

Part one of the first series of tests will explore the accuracy of the hybrid testing algorithm described in detail above in the Generalized Implicit Hybrid Testing Algorithm section of this report. These simulations will be completed using a linear numerical structural model with the damper also functioning in its nearly linear range. It should be mentioned that under these conditions the CU hybrid integration scheme remains configured to use 10 Newton iterations at each integration time step. This provides for a high level of accuracy and allows for the fact that the MR Damper is not a truly a linear damping device even with the velocity amplitude limited to its non-yielding range as can be seen clearly in Figure 19.
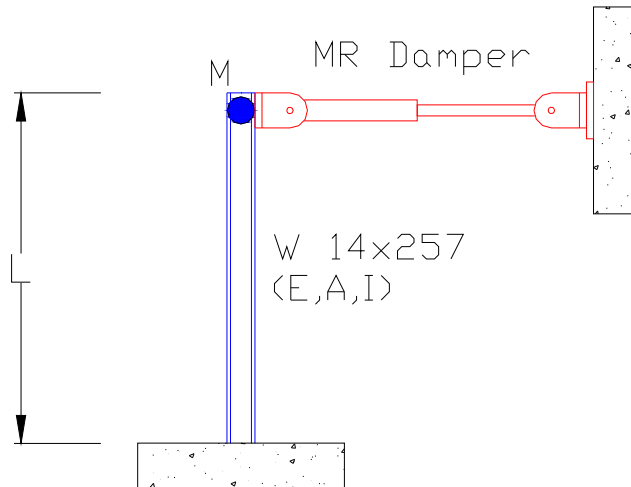
Figure 21: Hybrid Structural Model for Impulse Response Tests

The single column model described earlier is modified slightly with the length the column and the concentrated mass at the top treated as a variables. The FHT results obtained are compared directly to accurate fully numerical solutions. When the relative velocity of the two end points or nodes at each end of the MR damper are appropriately limited ($v_{max} \leq 0.3$ inches/second) the force-velocity response for the MR is similar to, but not exactly, that of an idealized linear viscous damper.

These algorithm accuracy tests will be conducted using a scaled horizontal base impulse function for excitation with the scaling done to achieve the velocity limitation described above. A total of 12 impulse response tests are summarized here.

For these tests consider the representation of the governing system of equations expressed in uncoupled or modal form where there are i modes and the equation of motion for each mode may be expressed as

$$\ddot{x}_i + 2\omega_i\zeta_i\dot{x}_i + \omega_i x_i = f_i \qquad (i = 1,2,3) \qquad \textbf{Equation 23}$$

This structures undamped fundamental flexural mode is dependant on the mass and flexural stiffness of the column. For these tests the damping during the hybrid simulations will be entirely due to the MR damper and the average linear initial damping values established for the three frequencies of the system ID tests will be used for the fully numerical simulation.

To investigate the accuracy of the FHT integration procedure under a variety of conditions the values of ω and ζ for the first bending mode will be varied and tested for the corresponding hybrid structure. In order to do this the length of the column and the discrete mass at the top of the column will be calculated for three different frequencies $(\omega = 2\pi, \pi, 0.2\pi)$ and 4 different damping values $(\zeta = 0.02, 0.04, 0.08, 0.16)$. The results from these hard realtime hybrid simulations are compared to accurate purely numerical simulations providing a basis for evaluating the accuracy of the FHT scheme. For the pure numerical simulations a linear viscous damping element will be used in place of the MR damper.

		M	L	ΔT for Corrected Natural frequency
$\omega_n = 2\pi$ $C_i = 43.6$	$\xi = 0.02$	173.5	35.1	0.000503
	$\xi = 0.04$	86.7	44.2	0.001006
	$\xi = 0.08$	43.4	55.7	0.002012
	$\xi = 0.16$	21.7	70.2	0.00403
$\omega_n = \pi$ $C_i = 57.6$	$\xi = 0.02$	458.4	40.3	0.000503
	$\xi = 0.04$	229.2	50.8	0.001007
	$\xi = 0.08$	114.6	64.0	0.002014
	$\xi = 0.16$	57.3	80.6	0.004027
$\omega_n = 0.2\pi$ $C_i = 66.2$	$\xi = 0.02$	2.634e+003	65.8	0.000503
	$\xi = 0.04$	1.317e+003	82.9	0.001006
	$\xi = 0.08$	658.5	104.4	0.002011
	$\xi = 0.16$	329.3	131.5	0.00402

Table 7: Model Properties for Damping and Natural Frequency Values

The values shown in Table 7 summarize how the model properties of column length and mass (L and M as shown in Figure 21) are varied to provide the desired natural frequency

and percentage of critical damping. The results of corresponding hybrid and pure numerical simulations are shown below.
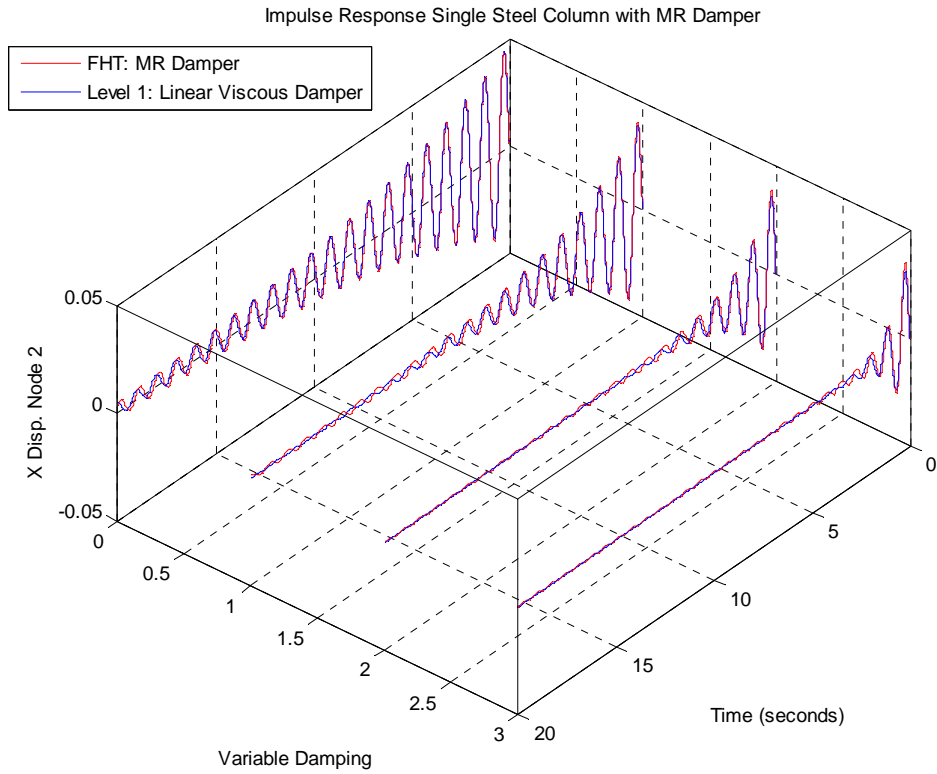

Figure 22: Impulse Response for Mode #1 Frequency = 1 Hz.
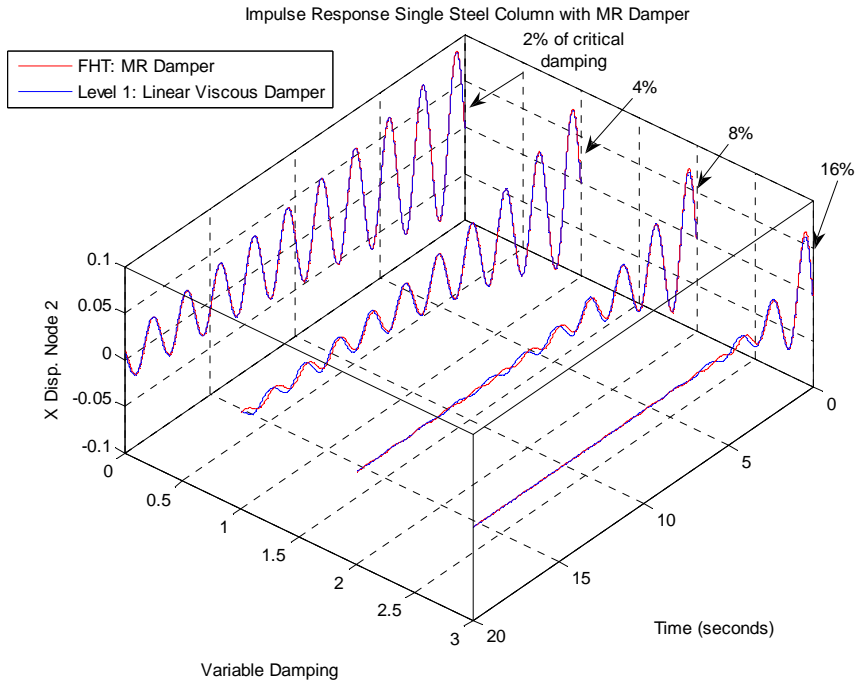
Figure 23: Impulse Response for Mode #1 Frequency = 0.5 Hz.
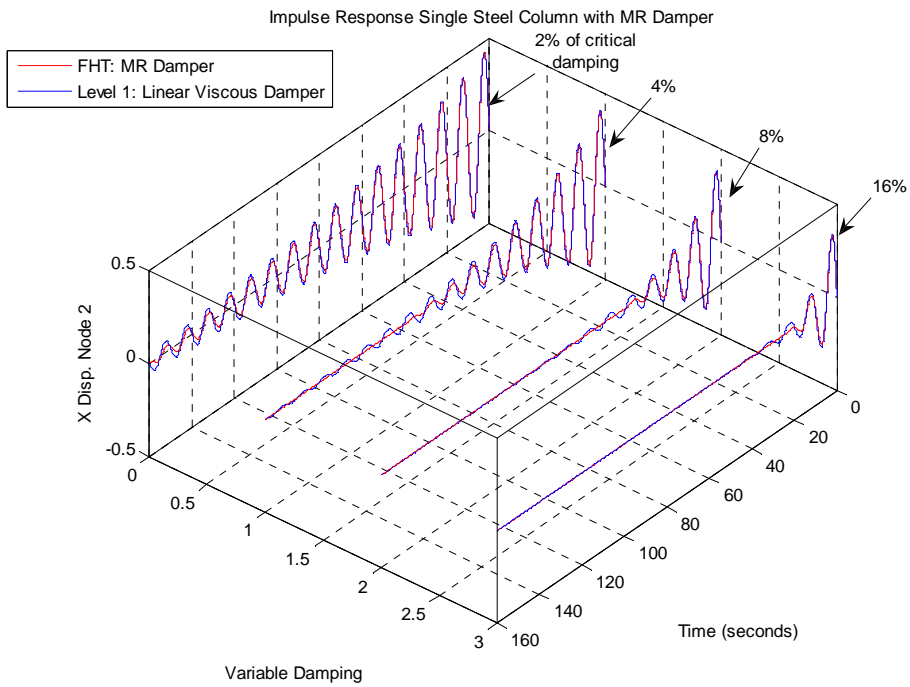
Figure 24: Impulse Response for Mode #1 Frequency = 0.2 Hz.

As is most apparent in Figure 22 and Figure 23 there is a small reduction in the period of oscillation for the hybrid simulation. This reduction increases as the damping is increased.

8.7 Significance of Actuator Phase Lag

In most closed loop hydraulic control systems there is a slight delay in the actuators response to a command signal. This delay can be easily quantified by directly comparing the actuator command and response curves during a hybrid or other type of simulation. It can be shown that this delay or phase lag will have the undesirable effect of adding apparent negative mass to the system. This is similar to how delay has been shown to result in negative damping for a stiffness based experimental component[10]. This can be seen most clearly by considering the simple scalar hybrid structure shown below where the classical single DOF linear oscillator is broken into a numerical component made up of mass and stiffness and an experimental component consisting of only a viscous damper. In a hybrid simulation ideally the value of x_n and x_e are exactly the same indicating perfect actuator performance, unfortunately this is very rarely the case.
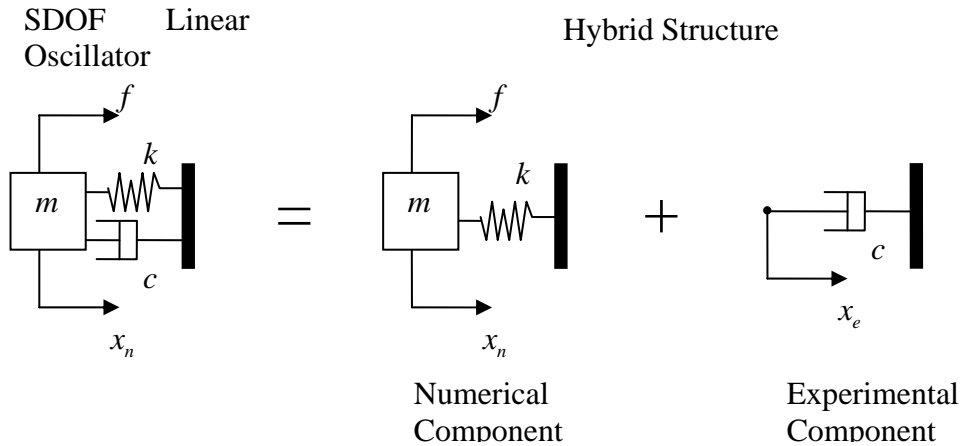
Figure 25: Idealization for a Hybrid Single Degree of Freedom Linear Oscillator

The equation of motion for the hybrid structure shown in Figure 25 is

$$m\ddot{x}_n + c\dot{x}_e + kx_n = f .$$ **Equation 24**

The relationship between x_n and x_e is taken from the experimental data where it is seen that there is a delay of δt seconds between these two values such that

$$x_e = x_n(t - \delta t)$$ **Equation 25**

The experimental velocity is now linearly approximated as

$$\dot{x}_e = \dot{x}_n(t - \delta t) \approx \dot{x}_n(t) - \delta t \cdot \ddot{x}_n(t).$$ **Equation 26**

With this approximation the equation of motion may be expressed in terms of only x_n

$$(m - c\delta t)\ddot{x}_n + c\dot{x}_n + kx_n = f.$$ **Equation 27**

The actuator delay results in an apparent negative mass. This result will prove to be useful in a subsequent series of these benchmark tests but also serves to explain a portion of the frequency distortion that takes place in the impulse response tests detailed above. An apparent reduction in mass due to actuator delay will decrease the period of the hybrid structure's fundamental mode. More damping or more delay results in further frequency distortion which is consistent with the trends observed in Figure 22 and Figure 23.

Upon closer inspection it is clear that this only partially accounts for the frequency distortion seen in these impulse tests. A typical value for δt during these tests is approximately 3 to 4 milli-seconds. The last column of Table 7 shows the change in the value of the period of oscillation, ΔT, for each of the impulse tests. These values explain a portion of the difference of same values determined graphically from the impulse response figures. The remaining portion can be attributed to the fact that the parameters used for the damper model (c_d and k_d) are determined from the full amplitude system ID tests when the maximum velocity is 0.3 inches/second. During the early part of the impulse response, when t is close to zero and the peak velocities are close to 0.3 inches/second, the FHT and pure simulation results match very nearly exactly. As the peak velocity drops during the later part of the impulse response there is some deviation from the pure simulation results.

In summary it is understood that these are demanding and revealing tests. A good level of accuracy has been demonstrated over a reasonably broad range of the vast possibilities with the acknowledgement that improvement is always needed and desirable.

8.8 Series 1: Accuracy and Model Size

The second part of the first series involves determining the maximum size of the numerical model that may be used in a hard realtime hybrid simulation. This is done by constructing a linear 3 story by 4 bay hybrid frame structure that will successfully run in hard realtime and then successively adding additional stories concluding with an n story by 4 bay steel frame structure where n is the largest possible integer value that is

permitted given hard realtime simulation conditions. The first structure tested in the model size series is a 3 story 4 bay model with the MR Damper connected diagonally in the second bay of the first story in the same location shown in Figure 27.

For each of these multi-story 4 bay tests the hybrid structure is base excited with a scaled version of the El Centro ground motion. The scaling is selected so as to limit the maximum velocity to less than 0.3 in/second at the connection node for the MR Damper. This avoids the strong nonlinearity in the force-velocity behavior of the MR Damper and allows for a more realistic direct comparison between the fully numerical level 1 simulations and the hybrid simulations involving the MR damper.

All of the models in this series have 4 percent Raleigh damping for the first and third modes of the structural model. The effects of the MR damper are superimposed on this base level of structural damping.

The horizontal response of the damper connection point (node #6) and the top story (node #4) for the 3 story 4 bay steel frame structure are shown in Figure 26. As expected the displacement response of the damper free structure is larger than both the Hybrid simulation involving the MR damper and the fully numerical simulation with an equivalent numerical viscous damper in place of the MR damper. The displacement response for the two damped structures (the blue and green curves) match quite well with very minor differences that, in all likelihood, can be attributed to differences between the velocity limited MR damper and a perfectly linear viscous damper. These differences include; 1) the equivalent best fit viscous damping coefficient (C_d) for the MR damper is velocity dependant while for the numerical damper it is fixed and constant and 2) there is inevitable line noise on both the displacement and force signals that come from the actuator and are digitized.
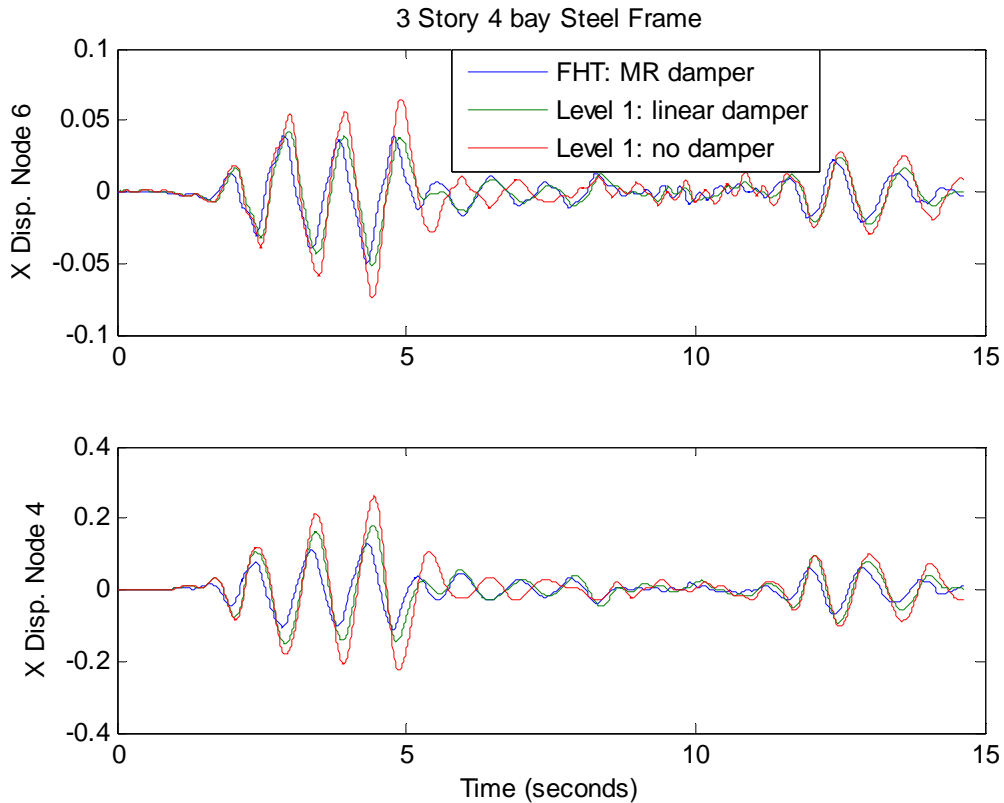
Figure 26: 3 Story 4 Bay Steel Frame Structure – Damper and Top Story Response

The model size series of tests culminated with a successful hard realtime simulation involving a 9 story 4 bay frame structure. This model has a total of 135 degrees of freedom. This simulation utilized the ten step Newton iteration procedure described above and in the process admits nonlinear behavior from the experimental component.

Once again the horizontal response of the damper connection point (node #6) and the top story (node #46) for the 9 story 4 bay steel frame structure are shown in Figure 27 and a similar quality of response is observed. Not to surprisingly the top story response shows very little difference for the 3 cases presented.
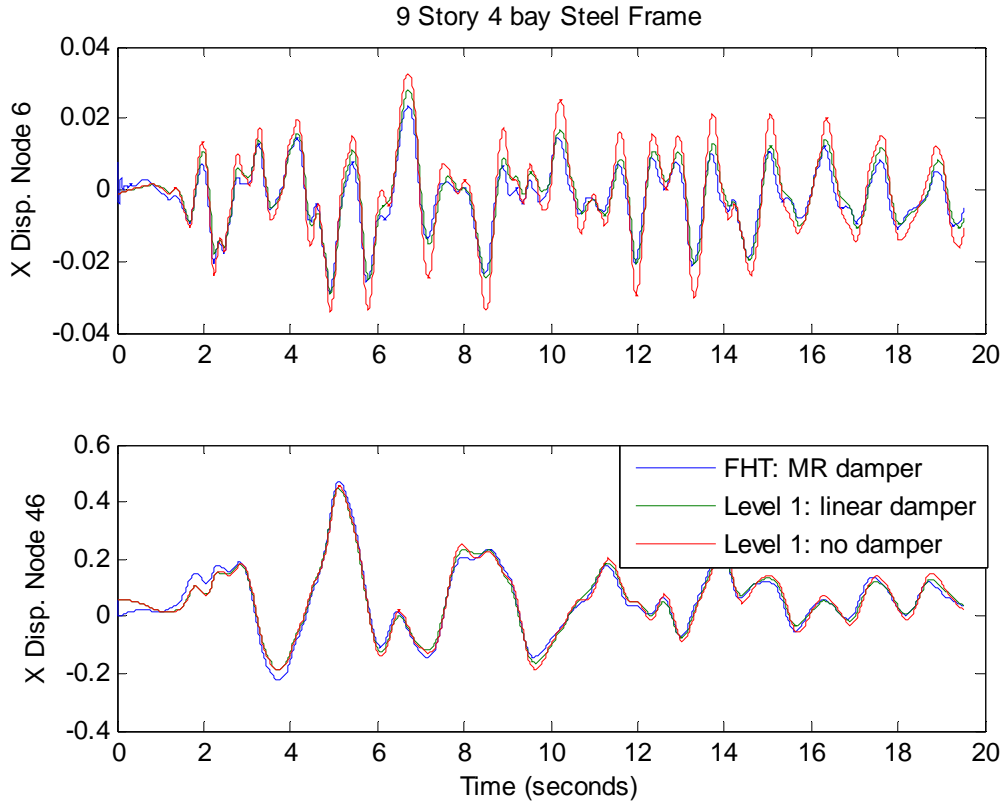
Figure 27: 9 Story 4 Bay Steel Frame Structure – Damper and Top Story Response

The largest structure that can be integrated in hard realtime is illustrated in Figure 28 with each beam and column identified. It is important to understand that this test was completed without a single violation of the strictest of hard timing constraints. In other words every single integration interval ($\Delta t = 0.009765625$ seconds) was completed on time and every single iteration interval ($\delta t = 0.0009765625$ seconds) was also completed on time. These are not averages nor are they distorted or misrepresented in anyway. All the way down to the millisecond level the one-to-one scaling of simulation time with actual testing time has been maintained and held constant from the beginning of the simulation to the end. The importance of this for hybrid simulations involving a rate sensitive device such as the MR damper will be made clearer in series 4 of these benchmark tests.

Also worthy of note is that the realtime target computer for all of these tests is an ordinary relatively inexpensive 5 year old Intel Pentium based Dell computer. Table 8 provides a detailed summary of the specifications and performance data for the target computer used for all of these benchmark tests. The processor is an Intel Xeon CPU running at 2.19 Ghz with 512 MB of RAM.

Matlab Benchmark Execution Speed	
Item	Execution Time
LU: LAPACK, n = 1000 - Floating point, regular memory access	0.3266
FFT: Fast Fourier Transform - Floating point, irregular memory access	0.6985
ODE Ordinary diff. eqn. Data structures and M-files.	0.4737
Sparse: Solve sparse system - Mixed integer and floating point.	0.6983
2-D: plot(fft(eye)) – 2-D line drawing graphics.	0.8704

Table 8: Specifications of Realtime Target Computer

The average results of ten executions of the Matlab Version 7.3.0.267 (R2006b) benchmark function are summarized in Table 8 and can be used to compare to other computers running the same benchmarks and version of Matlab.
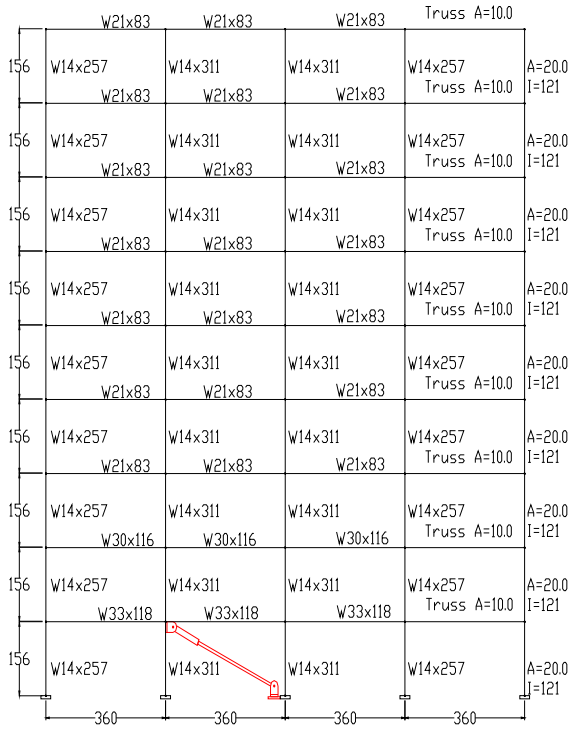

Figure 28: Large Model – 9 Story 4 Bay Frame Structure

8.9 Series 2: Model Behavior – Linear and Nonlinear

The second series of tests will progress systematically from the linear case of series 1 to the fully nonlinear case in which both the numerical structural model and the MR damper

are pushed into there respective nonlinear ranges. All of the series 2 simulations are completed in hard realtime. Attention is focused on and limited to the two benchmark hybrid structures described earlier. The single column steel structure and the 2 story 2 bay steel frame structure are each modeled in the linear case with only linear elastic beam-column elements. For the nonlinear numerical models all column elements are modeled with force-based nonlinear beam-column elements and the beams are all modeled with the beam-with-hinges element. Details for the fiber arrangement of the column elements and other relevant parameters may be found in the model description located in Appendix A. Both of these models are simplified versions of the so called SAC structure[11].

Single Column Model		Numerical Structural Model	
		Linear	Nonlinear
MR Damper	Linear	Level 1: (Figure 29) FHT: (Figure 29)	FHT: (Figure 29)
	Nonlinear	FHT: (Figure 30)	FHT: (Figure 30)

Table 9: Simulations for the Model Behavior Series – Single Column Structure

For the single column structure Table 9 provides an overview of the collection of tests conducted to investigate the linear and nonlinear behavior for this hybrid model.
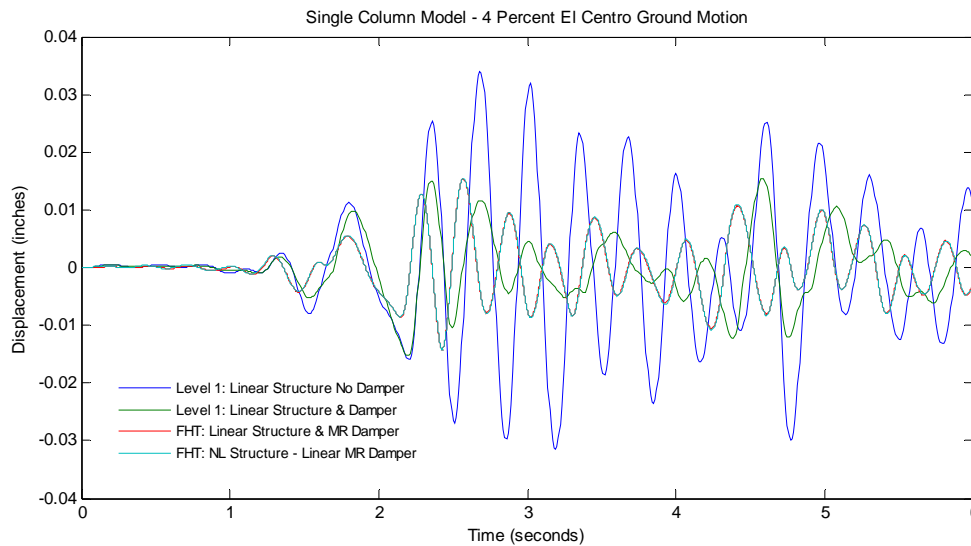

Figure 29: Hybrid Model Behavior – Linear Range of Damper

In Figure 29 the column top displacement histories are shown for both the linear and nonlinear structures models with the damper velocity limited to its nearly linear range. For the two hybrids tests involving the linear and nonlinear structure the responses match

nearly exactly. This is to be expected as the base excitation for both tests is identical and the nonlinear model is not pushed into any significant nonlinear behavior at this low level of excitation.

It is also apparent in Figure 29 that there is a slight shift in the damped natural frequencies of the structure. The no damper case (shown in blue) is subject to only Rayliegh damping which is set to 6.7 percent of critical. When the visco-truss damper is added (the green line) the percent of critical damping is increased to a total of 27 percent of critical. The calculated values for the damped and undamped natural frequencies are summarized in Table 10 below. These values are calculated using the equation

$$\omega_d = \omega_n (1 - \zeta^2).$$ **Equation 28**

Where ω_n and ω_d are the undamped and damped natural frequencies respectively and ζ is the viscous damping factor which indicates critical damping when $\zeta = 1$ (no oscillation for the unforced case).

Mode #	Undamped Case (Frequency in Hz.)	6.7 % Rayliegh Damping Only (Frequency in Hz.)	Rayliegh and MR Damper (Damped Frequency in Hz.)
1	3	2.9996	2.928
2	32.7	32.65	32.65

Table 10: Single Column Natural Frequencies

The first mode is affected by the addition of the MR damper as the percentage of critical damping is significantly increased. The second mode in this case (involving vertical vibration) is unaffected by the addition of the damper as the damper is oriented orthogonally to the motion.

The difference seen in Figure 29 between the level 1 simulation with the linear visco-truss element and the 2 FHTs with the MR damper is attributed to: 1) The frequency dependence of the damping coefficient for the MR damper while the visco-truss provides a damping coefficient that is independent of frequency, 2) The MR damper is not a perfectly linear viscous damper even when the velocity input is appropriately limited.

The Series 2 tests on the single column are concluded with strong ground motion (100% of the El Centro ground motion record) forcing the MR damper into the nonlinear range. It is interesting to note that the nonlinear column model results show significantly smaller velocity demands on the hydraulic actuator than the linear column model. This is most likely due to the increase in the energy that is absorbed by the nonlinear structure.
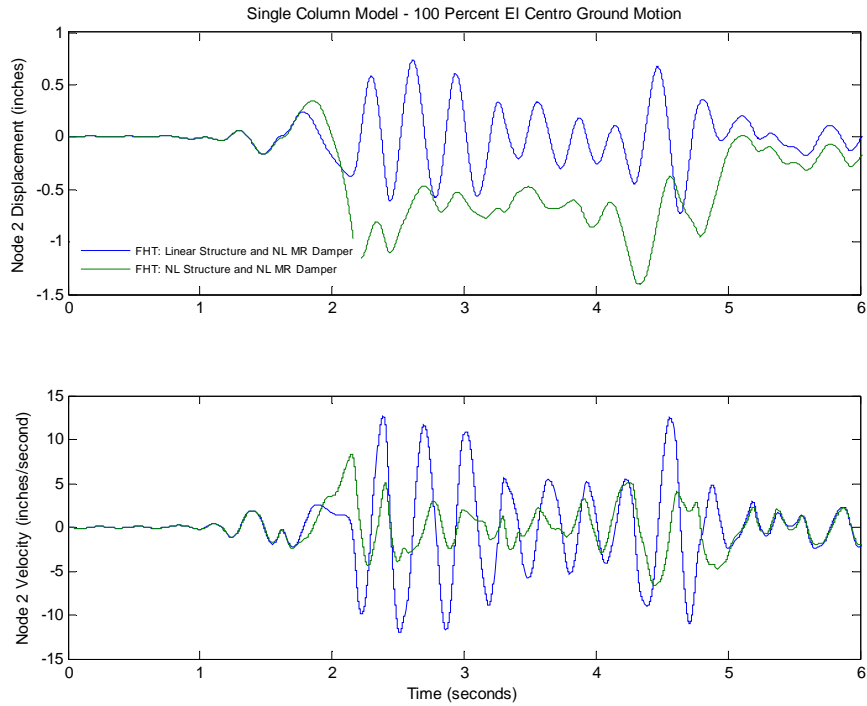
Figure 30: Hybrid Model Behavior – Nonlinear Range of Damper

In the case of the 2 story 2 bay frame structure similar trends are observed. In both cases the hybrid simulations with the linear structural model match nearly exactly the nonlinear model. This is not unusual as the ground motion has been reduced significantly (5% of El Centro) in order to maintain approximate linear behavior in the MR damper and in so doing the structure response is also limited to linear behavior even though a nonlinear model is employed.

2 Story 2 Bay Model		Numerical Structural Model	
		Linear	Nonlinear
MR Damper	Linear	Level 1: (Figure 31Figure 29) FHT: (Figure 31)	FHT: (Figure 31)
	Nonlinear	FHT: (Figure 32)	FHT: (Figure 32)

Table 11: Simulations for the Model Behavior Series – 2 Story 2 Bay Structure
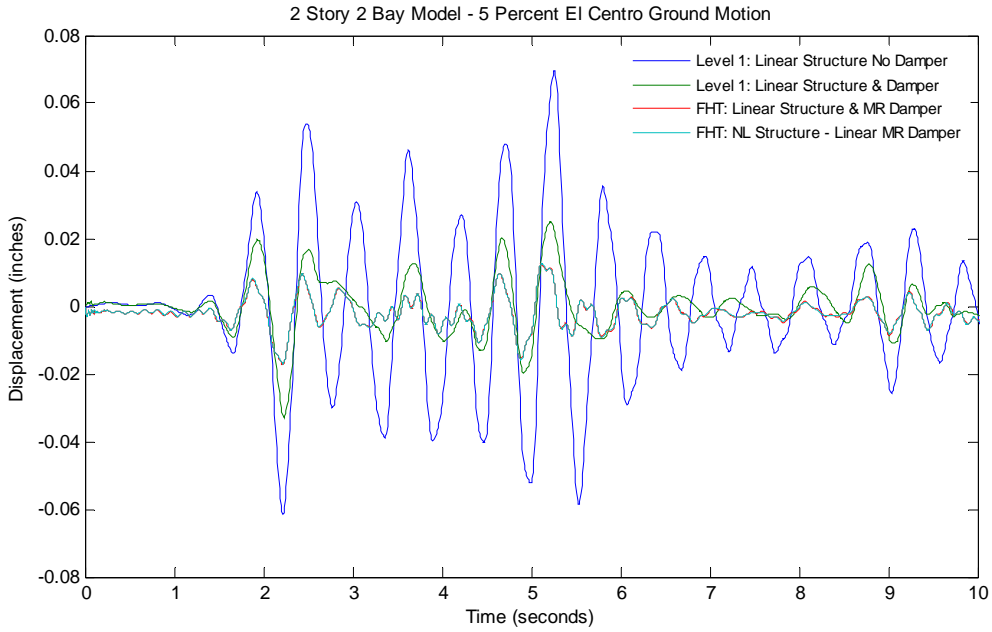
Figure 31:   Hybrid Model Behavior – Linear Range of Damper
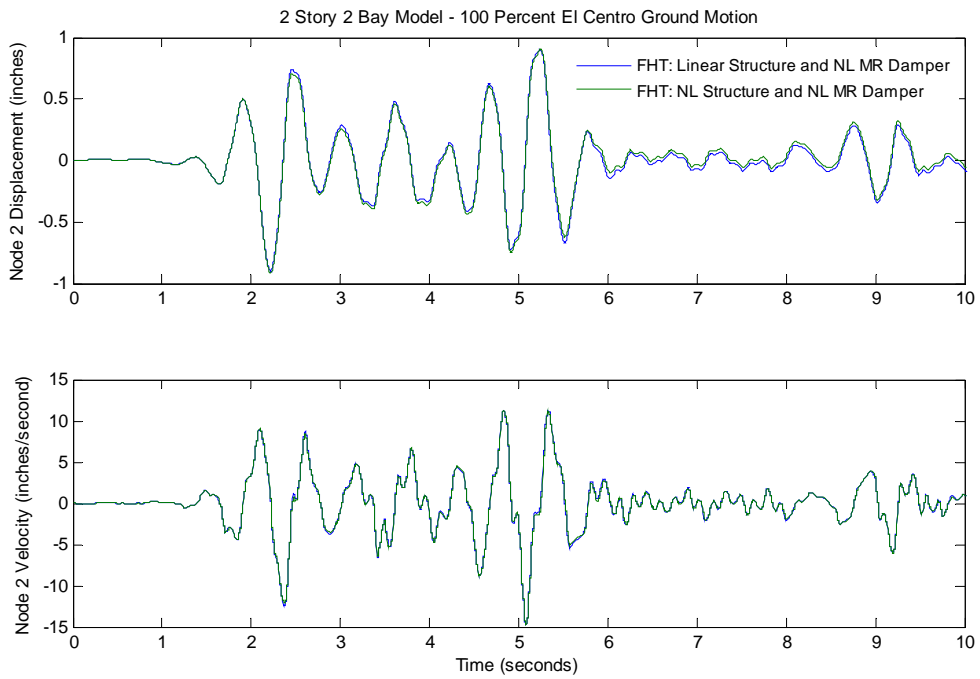
Figure 32: Hybrid Model Behavior – Nonlinear Range of Damper

56

A very useful and insightful capability of the CU NEES hybrid testing system is the ability to record the norm of the equilibrium residual throughout the simulation. Convergence to equilibrium during the Newton iteration process is indicated by the norm of the residual approaching zero.

In addition to systematically extending the linear simulations of the first series of benchmarks into the nonlinear range these results also provide a set of baseline responses for the 3 remaining series of benchmark tests.

8.10 Series 3: Actuator Performance

The third series of tests addresses some of the limitations relevant to hybrid testing for hydraulic actuators. Four tests have been carried out on both of the benchmark structures used in the series 2 tests, the single column and 2 story 2 bay frame structures.

The first of the four tests is at very low excitation amplitude. Both structures are base excited with 0.26 percent of the El Centro ground motion. Figure 33 compares the expected response calculated from a level 1 fully numerical simulation with a FHT.
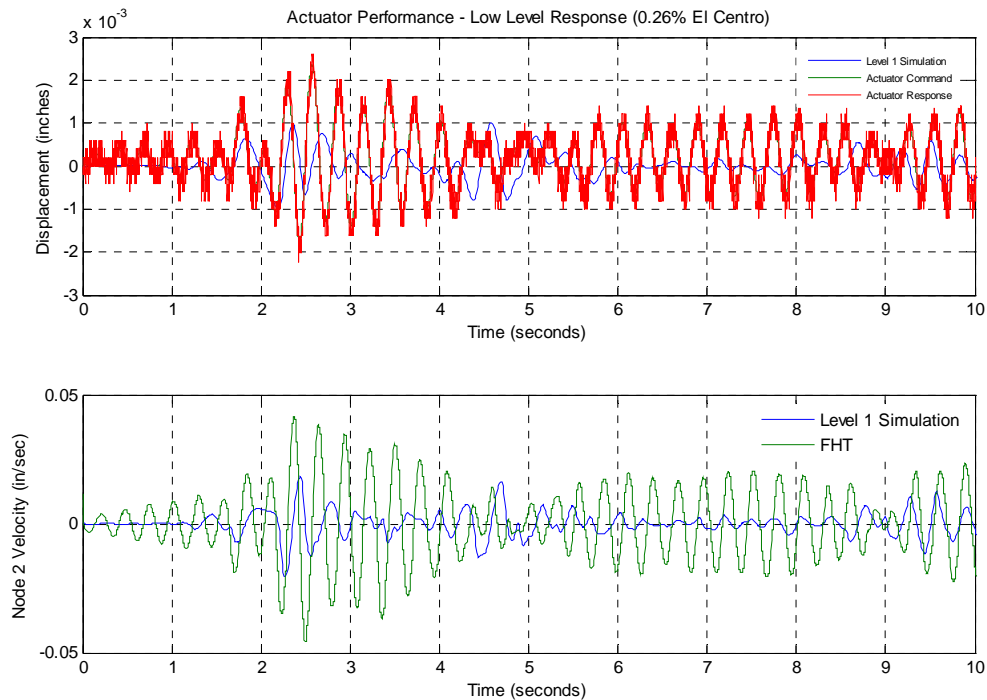
Figure 33: Actuator Performance Single Coulmn Model – Very Low Level Excitation/Response

The peak velocity is well within the range of the nearly linear response of the MR damper so we would anticipate that the level 1 simulation matches reasonably well with the FHT.

This is not the case and can be attributed to inaccuracies arising from a poor Signal to Noise Ratio (SNR). The SNR for the actuator's internal LVDT is approximately 0.568 where the SNR is calculated using

$$SNR = \left(\frac{A_{signal}}{A_{noise}} \right)^2$$

Equation 29

and A is the RMS amplitude of the signal. The same difficulty can be seen in Figure 34 for the 2 story 2 bay model.
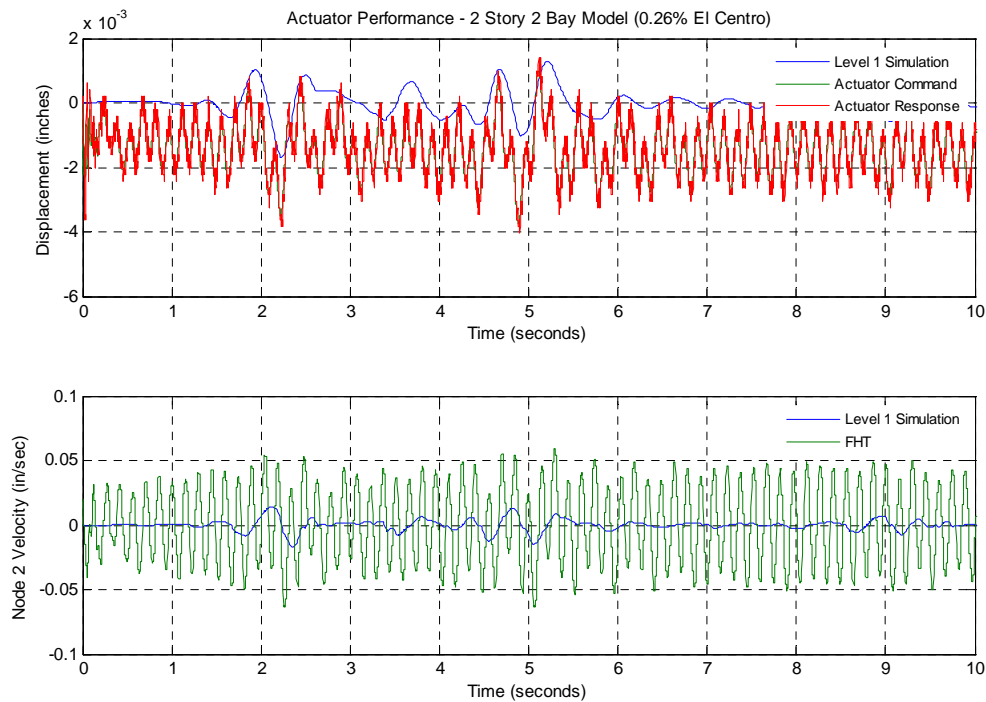
Figure 34: : Actuator Performance 2 Story 2 Bay Model – Very Low Level Excitation/Response

As the level of base excitation is increased the SNR improves significantly, with the El Centro base motion scaled to 10 percent the signal to noise ratio increases to 2160. For both models the expected response is only a few thousandths of an inch so it's not that surprising that the fidelity of hybrid simulation is fairly poor. It is reassuring to see that under these conditions stability is not an issue.

In the final three tests of the series our attention is now shifted to the phase lag that results as the actuator motion approaches its velocity limit. This occurs as the scaling of the base motion is increased.
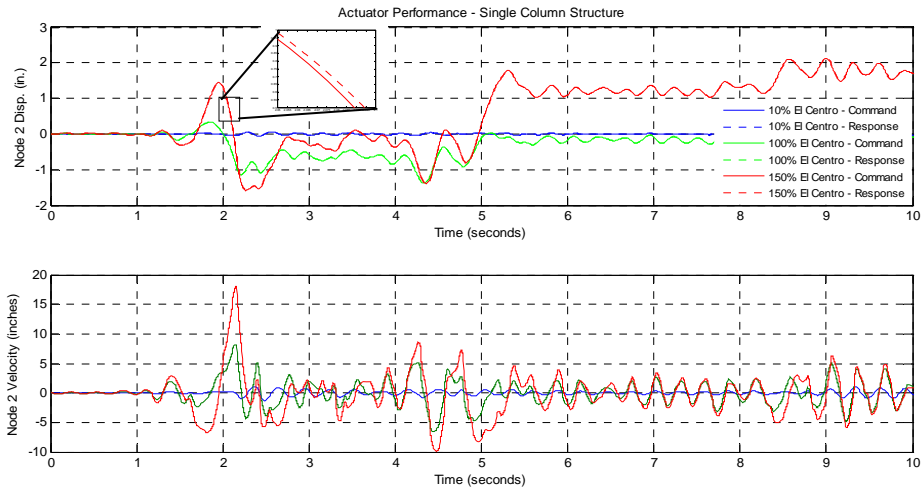
Figure 35: Actuator Performance Single Coulmn Model – Increasing Excitation

With the MTS control system aggressively tuned for maximum performance a phase lag is still readily observed in these tests. This can be seen most clearly at the velocity peak that takes place just after 2 seconds into the simulation. This region of time is enlarged in Figure 35 to illustrate delay in the actuator response. A summary of the observed actuator delay is provided in Table 12 illustrating that increased actuator velocity results in an increased command-response phase lag despite being well within the maximum velocity of the actuator (in this case 20 inches/second).

Actuator Command-Response Delay (milli-seconds)		
Percent Scaling of Ground Motion	Single Column Model	2 Story 2 Bay Model
0.26	0	0
10.0	2	2
100.0	4	3
150.0	6	5

Table 12: Actuator Performance and Phase Lag

The analysis provided on page 47 indicates that as the phase lag increases there is a corresponding increase in negative apparent mass that has a potentially destabilizing effect. Indeed, as we shall see in the 5th and final series of benchmark tests, when the initial damping coefficient is very large difficulties arise. Application of the force correction in Equation 17 should resolve this problem but this is yet to be implemented and tested.

8.11 Series 4: Hard & Soft Realtime

The realtime series of tests will investigate the effects of compromising the condition of hard realtime during hybrid simulations involving the MR damper. By distorting the scaling of time in a variety of ways during a hybrid simulation the importance of correct time scaling is explored.

For the simulations involving the 2 story 2 bay model attention is focused on the element force data for element number 2 (the center first story column). Because the applied ground motion is in the horizontal direction results will be presented for the global x direction element force as well as the moment.

If creating the conditions for conducting hard realtime hybrid simulations is an unneeded luxury than one would expect that simulation data from time distorted simulations would be a reasonable and perhaps even accurate representation of the actual conditions and response obtained under hard realtime conditions. With this in mind we consider that the time distorted simulations should be bracketed in a sense by two differing simulations. On the one hand an accurate result is provided by the hard realtime simulation using implicit time integration and conversely an undesirable result is provided by the solution obtained with no damper element at all. These two cases provide a bound or range within which the various soft realtime simulations vary. Due to the nonlinear behavior of both the numerical model and the MR damper these two responses provide more of a conceptual upper and lower bound and not an absolute one.
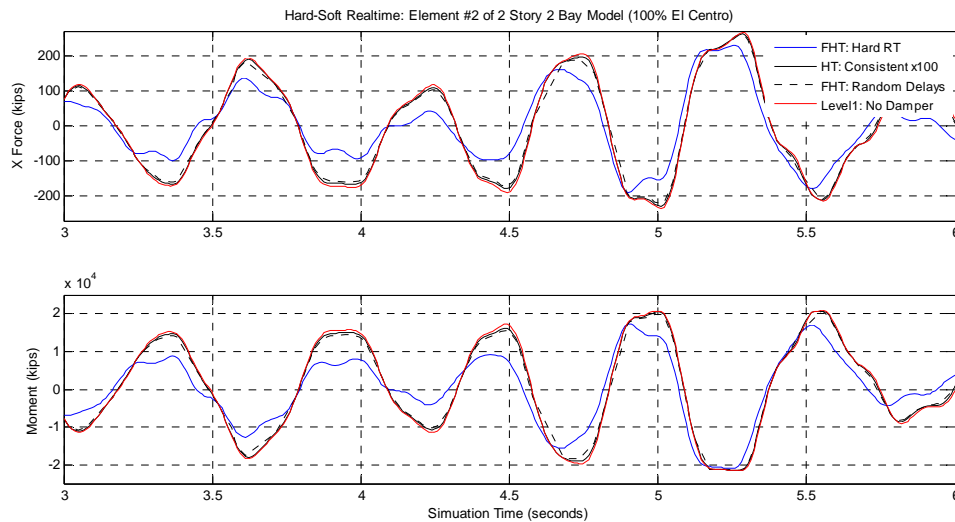

Figure 36: Hard-Soft Realtime – Element Force Data Using Implicit Time Integration – Base of 1st Story Center Column

For the case of consistently scaled time that expands uniformly, the duration of the simulation by a factor of 100, it is clear from Figure 36 that the response is significantly effected by the distortion of simulation time. Indeed the response for the element force

data nearly traces exactly the no damper case indicating that the damper is very nearly unaccounted for throughout the simulation. This is certainly not the intention nor a desirable attribute of hybrid simulations.

The next variation of time scaling imparts a random component to the distortion of the time scale. This can be thought of as either a random communication delay that takes place during point to point geographically distributed testing or the variations in computation time that might result from the use of a non realtime operating system. This is not intended to be an exact replication of either of these conditions, merely an approximation of such conditions.

The dashed black line in Figure 36 is the result of programming a random delay at each computation cycle ranging from zero to 200 milliseconds. Again it is observed that the cost of compromising the conditions of hard realtime is very severe as the random time distorted response nearly matches the damper free response.

Two additional soft realtime simulations were carried out both using explicit time integration (Alpha Operator Split) and the OpenFresco hybrid simulation software developed at the University of California Berkley. The results shown in Figure 37 utilized the interpolation and extrapolation feature that is implemented in the 2007 distribution of OpenFresco.
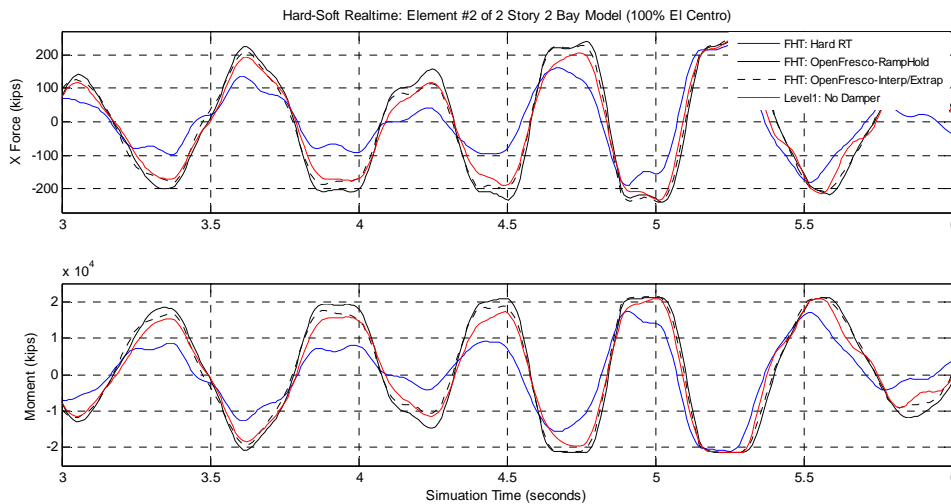
Figure 37: Hard-Soft Realtime – Element Force Data from Explicit Time Integration – Base of 1st Story Center Column Element

The other simulation utilizing explicit time integration was obtained using conventional ramp and hold command generation. This was done by replacing the interpolation-extrapolation logic in OpenFresco with a conventional linear ramp and hold.

A summary of the soft realtime results are presented in Figure 38. For each of the four variations of soft realtime a Hybrid Force Component Compliance (HFCC) factor is calculated using

$$HFCC_i = \frac{F_i^{SimSoft} - F_i^{NoDamper}}{\left| F_i^{HRT} - F_i^{NoDamper} \right|} \times 100 \qquad \textbf{Equation 30}$$

Where F_i^{HRT} is the ith element force value in the time history for the implicit hard realtime case which fully engages the hybrid experimental component, $F_i^{NoDamper}$ is the ith element force for the implicit solution that has no hybrid experimental component (the MR damper has been removed from the model) and $X_i^{SimSoft}$ is the ith solution for the simulation involving some alteration of simulation time. In an ideal situation the HFCC would have a value of 100 throughout a simulation indicating that the distortion of simulation time had no measurable effect on the element force. A HFCC value of zero is an indication that the simulation is not accounting for the presence of the experimental component at all. A negative value indicates a large error that reaches outside the boundary of the no damper case. In all cases very high levels of error are indicated as there are only brief instances for which the HFCC is even close to 100. The region of time shown in Figure 38 is very much typical of the values obtained throughout the duration of the simulation.
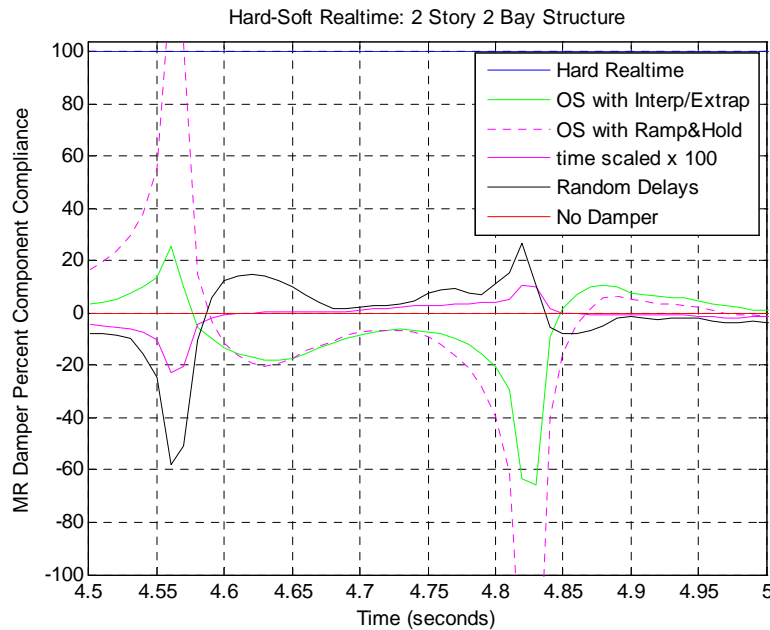
Figure 38: Hard-Soft Realtime and Hybrid Force Component Compliance

Means values for the HFCC in the time interval shown in Figure 38 are summarized in Table 13. That non of these values is even positive indicates the very real need for hard realtime simulation conditions for tests similar to these. In the case of the simulations done with the Operator Split integrator it is acknowledged that some portion of the error may be attributed to the integration method used.

Simulation Case	Mean HFCC
Random Delay	-0.78
Consistently Scaled (x100)	-0.88
OS Interp/Extrap	-5.29
OS Ramp and Hold	-5.59

Table 13: Hard-Soft Realtime: Mean HFCC for 4.5<t<5.0

A similar series of tests involving the single column structure also indicate the importance of maintaining and correctly scaling time (hard realtime) for hybrid simulations involving a nonlinear damping device such as the MR damper. In Figure 39 again bounds are provided by the accurate solution obtained under hard realtime conditions (the green line) and the damper free solution (the red line) using the implicit integration scheme. The two blue lines (solid for time scaled or expanded by 10 and dotted for time scaled by 100 times) are taken from consistently scaled time tests. The distortion or expansion of simulation time is uniform and consistent throughout the entire test. This is done using the same program and hardware as the hard realtime simulations with minor modifications allowing for the consistent expansion of testing time. As would be expected when the time scaling factor is reduced, from 100 to 10 in this case, the solution approaches the hard realtime result.
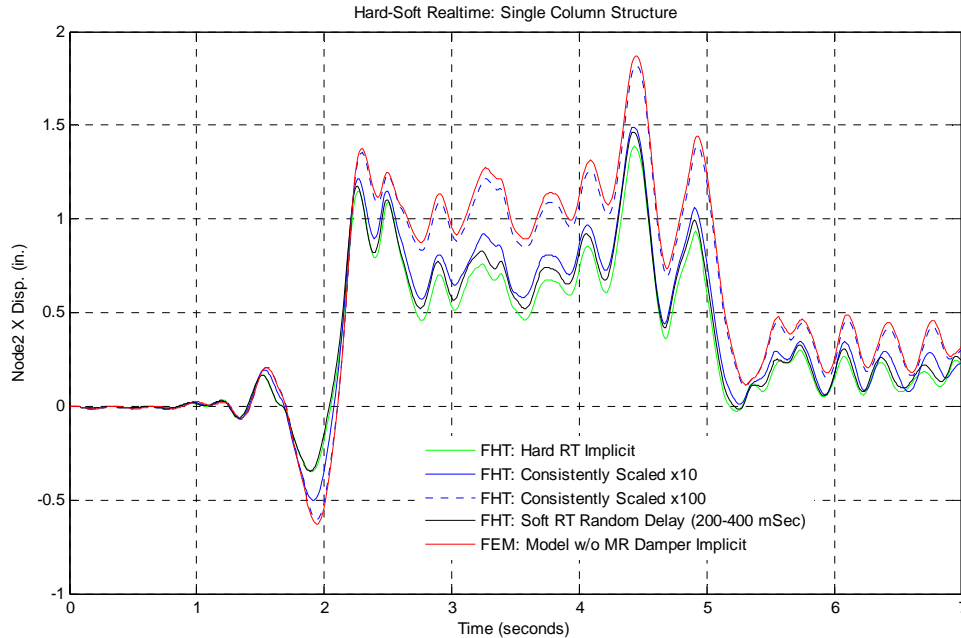
Figure 39: Hard-Soft Realtime – HHT Implicit Integration with Varying Time Distortion

A varying time distortion in the form of a random delay between 200 and 400 milliseconds that occurs at 0.2 percent of the computation cycles is shown in black.

Two additional cases for explicit time integration are also considered. Both involve the use of OpenFresco, the first with extrapolation and interpolation and the second using a series of rapid ramp and holds in place of the extrapolation and interpolation. The extrapolation/interpolation approach ideally provides a higher level of continuity[12] and was developed at the University of California Berkley by Gilberto Mosqueda. In the initial phase of the integration time step, during the computation of the next solution point, a command signal is generated that extrapolates forward in time based on prior solutions. Once the solution is available a transition to interpolation takes place. An event driven approach is used to implement this that accommodates a total of five states (extrapolate, interpolate, slow, hold, and free-vibration). OpenSees is used to carry out the computations for the α-operator split integrator on one computer, running under a non-realtime Operating System (OS), and the interpolation/extrapolation command generation is carried out on a second computer in a realtime computing environment.
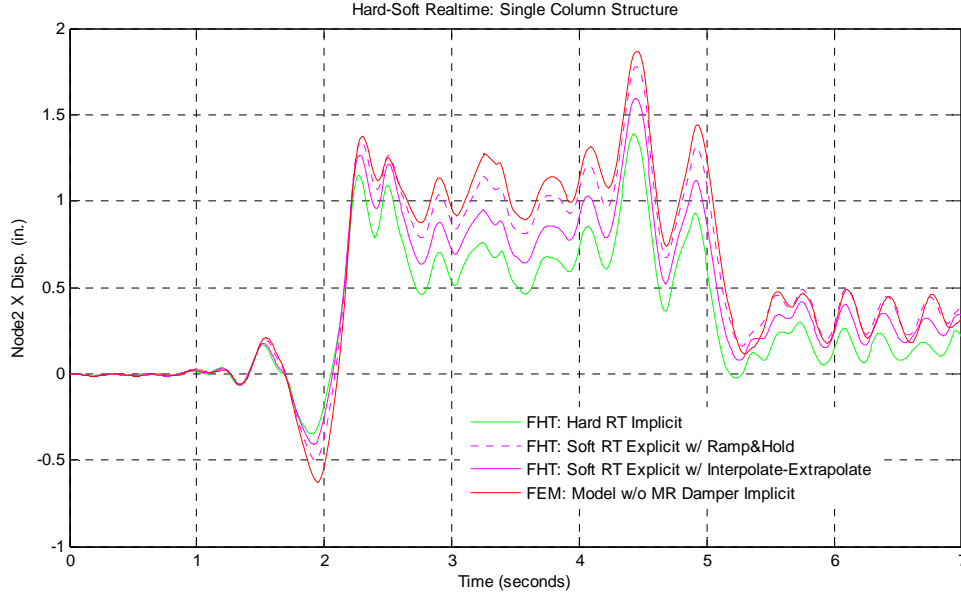
Figure 40: Hard-Soft Realtime – Explicit Alpha Operator Split Integration & OpenFresco

Figure 40 shows the improvement achieved by moving from a ramp and hold approach to the extrapolation and interpolation implemented in OpenFresco. For comparison purposes a Hybrid Component Compliance (HCC) factor is again defined. It is based on the two accurate solutions mentioned above obtained using implicit time integration. The HCC is calculated at each discrete instance of time throughout the simulation using

$$HCC_i = \frac{X_i^{SimSoft} - X_i^{NoDamper}}{\left| X_i^{HRT} - X_i^{NoDamper} \right|} \times 100 \qquad \textbf{Equation 31}$$

Where the X_i^{HRT} is the ith solution for the implicit hard realtime case which fully engages the hybrid experimental component, $X_i^{NoDamper}$ is the ith solution for implicit solution that has no hybrid experimental component and $X_i^{SimSoft}$ is the ith solution for the simulation involving some alteration of testing time deeming it a soft realtime simulation. A HCC value of 100 indicates full compliance and a solution that matches exactly the accurate implicit solution involving the damper. A value of 0 indicates a total lack of compliance and a solution the matches exactly the damper free simulation, certainly an undesirable condition with regard to simulation error. During the strong motion portion of the simulation, $(3 < t_{sim} < 5)$, the HCC is plotted in Figure 41 and graphically indicates that the solution with random time distortions provides the best level of accuracy. The mean value of the HCC for the various soft realtime cases is summarized in Table 14.
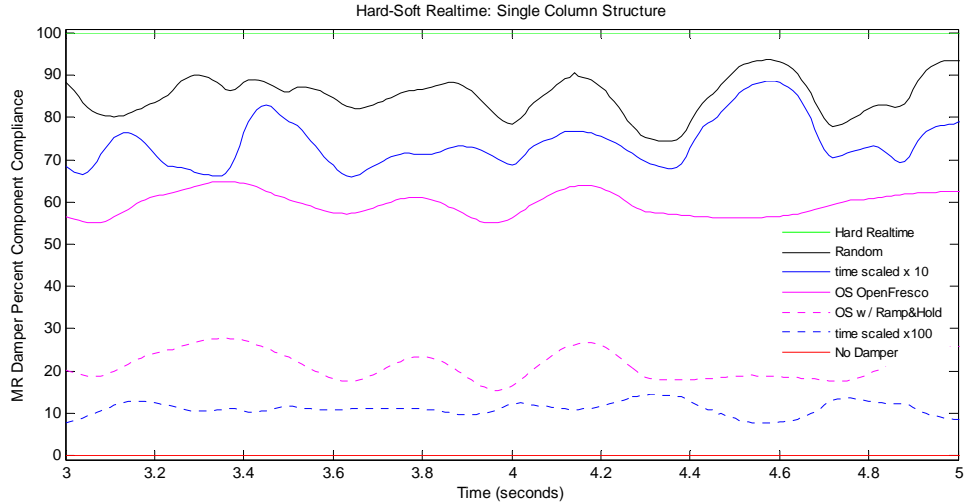
Figure 41: Hard-Soft Realtime – Experimental Component Hybrid Compliance Factor

For the simple single column structure the least distorted of the soft realtime cases studied here is the intermittent random distortion with a mean HCC of approximately 86. By most measures this is not an adequate level of accuracy and it is difficult to envision a research and testing scenario for which this level of accuracy is acceptable. It is also difficult to establish a priori that a given relaxation of hard realtime conditions will yield a result with sufficient accuracy.

Simulation Case	Mean HCC
Random	85.7
OS OpenFresco	59.4
Consistently Scaled (x10)	74.4
OS Ramp and Hold	21.1
Consistently Scaled (x100)	11.0

Table 14: Hard-Soft Realtime: Mean HCC During Strong Motion

8.12 Series 5: Relative Component Participation

The final series of tests will explore the effects of increasing the relative force component participation of the damper by scaling up the measured force signal from the actuator that is driving the MR damper. This implies that given a relative displacement and velocity pair ($x_{MRD}, \dot{x}_{MRD}$) describing the extension and velocity respectively of the MR damper's piston the measured resultant force is increased by n times.
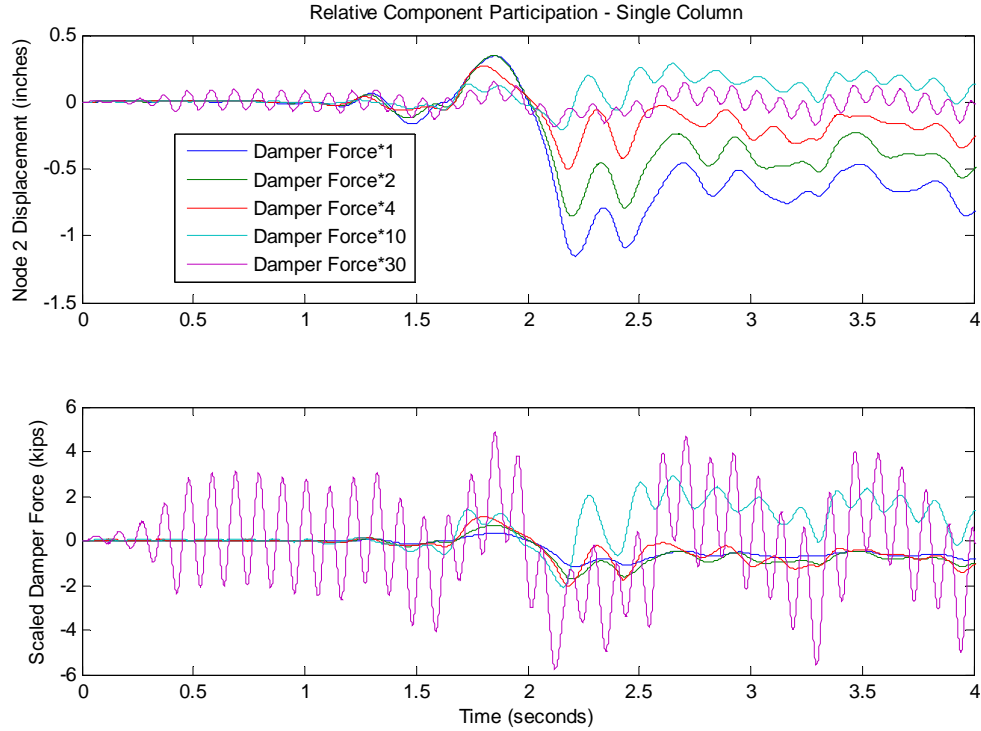
Figure 42: Relative Component Participation – FHT with 100% El Centro Ground Motion

The data shown in Figure 42 is generated using a hybrid model in which both the measured MR damper force and the estimated value of linear initial damping, C_i, are increased by the same amount. With these values increased by 30 times a persistent oscillation appears with a frequency of approximately 9.5 hz. This frequency does not coincide with any of the natural frequencies of the structural nor is it strongly present in the ground motion record. It is noted that the first mode for this structure is heavily over-damped under the conditions created by the scaled damping force of 30. The mass, damping and stiffness associated with the first mode are $m = 5.92$ $kslugs$, $c = 1,354$ $\dfrac{kips}{in./\sec.}$, $k = 2104$ $\dfrac{kips}{inch}$ and the viscous damping factor is

$$\varsigma = \frac{c}{2m\omega_n} = 6.06$$ **Equation 32**

This is more than 6 times critical damping so this structure will no longer freely oscillate. Figure 43 indicates that as the value for the linear initial damping, C_i, is increased with the force scaling factor held constant at 30 the oscillation in attenuated while the oscillation frequency increases slightly. This would appear to indicate the oscillation is associated with the numerics and not mechanics of this simulation. A problem very similar to this was also noticed during the NEESr research project directed by Prof. Christenson. The structure in this case is much simpler.
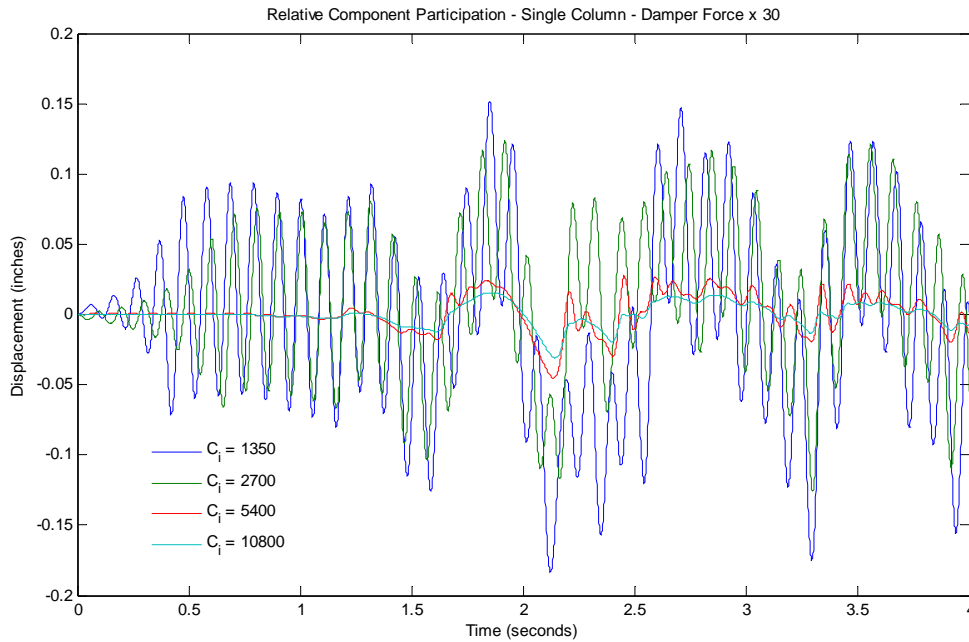
Figure 43: Relative Component Participation – FHT 100% El Centro with Force Scaling of 30

Recall the earlier analysis for a scalar liner oscillator where the actuator delay was shown to be equivalent to adding negative mass in the amount of $c \cdot \delta t$. Using the values for the fundamental mode and the observed actuator delay prior to the unset of the oscillation of 0.004 seconds the negative apparent mass is 5.41 slugs. This value is very close to the actual mass for the fundamental mode. For the scalar EOM a negative mass results in an imaginary natural frequency and conditions which or numerically intractable. This would explain the persistent oscillation that plagues this series of simulations. Efforts to adjust the MTS control for better performance and therefore reducing the actuator delay provided ineffective.

A very similar phenomena is observed in the case of the 2 story 2 bay model with the same trends observed and described above.

9 Summary

An overview of many of the important considerations and limitations involved in hybrid simulation at the CU NEES FHT facility has been provided here. Hybrid testing has the benefit of limiting the complexity and size of an experimental test component. It is apparent that this benefit comes at the expense of added simulation and laboratory technological demands. To this end the CU NEES FHT facility and its users benefit from the on-going support of NSF through NEES Inc. It does indeed seem unreasonable to expect every researcher and research project that uses hybrid testing techniques to

become thoroughly versed in the subtleties and demands of these techniques. Having said this, the benefits to a researcher of a more thorough and in depth understanding of the techniques and equipment involved are significant and important.

Due to the modular nature of the CU NEES FHT system it should be apparent that existing limitations due to a single component may be overcome by upgrading or expanding that component. The current testing equipment was procured and integrated into the overall system based on the expected demands of typical seismic events and research. In the time that this system has been in service it has performed very successfully in meeting the demands of the earthquake engineering research community.

Fast or RT hybrid testing is a relatively new research field that has benefited very tangibly from the technological advances that have accompanied our more and more digital and microprocessor oriented world. There has been a very real need in the past to alter the scaling of time in dynamic hybrid simulations due to both hard and soft technological limitations. These obstacles, for the most part, are no longer valid and the decision regarding whether or not to allow for the distortion of the relationship between prototype, simulation and testing time should be based on the importance of relevant material and devise rate effects.

10 Conclusions

The CU NEES FHT laboratory is a hybrid testing facility with strict hard realtime simulation capabilities. Experience with the unconditionally stable implicit direct time integration algorithm used at CU has confirmed the robustness and accuracy of this approach. Rate sensitive materials and devices such as the MR damper necessitate that hybrid simulations be carried out in hard realtime. The significant effects shown in this report of relatively minor time distortions on MR damper hybrid simulations highlight the need for a careful and accurate representation of time in the simulated event. One might be tempted to argue that there exists a gray area within which limited time distortions lead to relatively minor and acceptable errors. As researchers familiar with nonlinear systems know, there exists a very fine sensitivity of these systems to initial conditions and every effort must be taken to reduce sources of uncertainty and error. For researchers and engineers developing and testing new earthquake resistant materials, devices or designs, especially ones with demonstrated rate sensitivities, it is no longer necessary to work and conduct research in this gray area and hope for the best.

Current effort in our site centers around localization of OpenFresco and SIMCOR as well and the development of a streamlined computational environment for real time hybrid simulation which exploits latest hardware technology.

11 Acknowledgement

12 Appendix A: OpenSees Input Files 3 DOF Steel Frame FHT and Level 1 Simulations

Two Story Two Bay w8xs35 Benchmark Model #1

```
#
#       This is a tcl and fht script file for the first FHT benchmark
#       structure.  A 2 story 2 bay frame that is fully fixed at the base and
#       the exerimental element is the center column of the first story.
#
#       With minor changes this script can be modified to
#
#               1.  Run as a tcl input script for the standard release of OpenSees
#               2.  Run as a fht input script for the RT version of OpenSees developed
#                       at the CU Boulder FHT NEES laboratory
#               3.  A fully linear model
#               4.  A nonlinear model
#
#       These changes are easily made by altering the commenting of the appropriate
#       lines below
#
#
#       Modified 11-05-2007   EJS
#
#       Units: kip, in, sec

#model FHT -ndf 3 -ndm 2
model BasicBuilder -ndf 3 -ndm 2

node 1 0.0 0.0
node 2 0.0 50.0
node 3 0.0 100.0

node 4 75.0 0.0
node 5 75.0 50.0
node 6 75.0 100.0

node 7 150.0 0.0
node 8 150.0 50.0
node 9 150.0 100.0
```

```
mass 2 1.0 0.0 0.0
mass 3 0.5 0.0 0.0

mass 5 2.0 0.0 0.0
mass 6 1.0 0.0 0.0

mass 8 1.0 0.0 0.0
mass 9 0.5 0.0 0.0

fix 1 1 1 1
fix 4 1 1 1
fix 7 1 1 1

#according to mill report
uniaxialMaterial Steel01 1 35 29000 1e-6

#W8*35
section Fiber 1 {
patch quad 1 3 2       -4.06    4.01 -4.06 -4.01 -3.565 -4.01 -3.565 4.01
patch   quad 1 1 5      -3.565 0.155 -3.565 -0.155 3.565 -0.155 3.565 0.155
patch   quad 1 3 2 3.565 4.01 3.565 -4.01 4.06 -4.01 4.06 4.01
}


#Columns
geomTransf Linear 1

element nonlinearBeamColumn 1 1 2 4 1 1
element nonlinearBeamColumn 2 2 3 4 1 1

element nonlinearBeamColumn 4 5 6 4 1 1

element nonlinearBeamColumn 5 7 8 4 1 1
element nonlinearBeamColumn 6 8 9 4 1 1

#Beams
geomTransf Linear 2

element elasticBeamColumn 7 2 5 35.3 29000 1380 2
element elasticBeamColumn 8 5 8 35.3 29000 1380 2

element elasticBeamColumn 9 3 6 35.3 29000 1380 2
element elasticBeamColumn 10 6 9 35.3 29000 1380 2
```

#element sNodeElement 11 5 1 1 1 1 1 1 131.19 0 4135.83 0 967.65 0 4135.83 0
204128.4 1 0 0 0 -0.5 -0.5 0 0.01389 -0.01389 1 0 0 0 -1 36 0 -1 -36
element nonlinearBeamColumn 3 4 5 4 1 1

puts "eigen values prior to transient analysis: [eigen 3]"

recorder Node -file NL_F80_dt0p05.out -time -node 5 6 -dof 1 2 3 disp
#recorder Node FirstNonlinearTest.out disp -time -node 5 6 -dof 1
#recorder Node validationDisp.out disp -time -node 5 6 -dof 1
#recorder RealTimeNode DispRealTimeEBeams.out disp -time -node 5 6 -dof 1 -
numStep 4000 #Use -numStep>=analysis time steps

#recorder RealTimeNode validationDisp.out disp -time -node 2 5 8 3 6 9 -dof 1 2 3 -
numStep 4000 #Use -numStep>=analysis time steps
#recorder Node validationDisp.out disp -time -node 2 5 8 3 6 9 -dof 1 2 3
#recorder RealTimeNode validationVel.out vel -time -node 5 -dof 1 -numStep 1500
#Use -numStep>=analysis time steps
#recorder ElementPostAnalysis 1 -time   -file validationEle.out -numStep 1500
globalForce #Use -numStep>=analysis time steps

#max displ. =.. 0.5 inch.
#pattern UniformExcitation 1 1 -accel Path -filePath ElCentro -dt 0.01 -factor 80.0

#max displ.=0.61 inch.
#pattern UniformExcitation 1 1 -accel Path -filePath ElCentro -dt 0.01 -factor 170.0

#max displ. =.. 0.94
#pattern UniformExcitation 1 1 -accel Path -filePath ElCentro -dt 0.01 -factor 220.0

#max displ. =.. 2.1
#pattern UniformExcitation 1 1 -accel "Path -filePath ElCentro1.txt -dt 0.01 -factor
300.0"

pattern UniformExcitation 1 1 -accel "Path -filePath Elcentro1.txt -dt 0.01 -factor 80.0"
#pattern UniformExcitation 1 1 -accel "Path -filePath ElCentro1.txt -dt 0.01 -factor 80.0"

#converge test
tol   maxIter printFlag
test EnergyIncr 1.0e-30   20   5
constraints Plain

these values give 4 percent damping to modes 1 and 2
integrator Newmark 0.5 0.25   0.656911   0.0   0.0   0.0019992
#2% damping on first 2 modes according to w1=, w2=
#integrator FHT 0.5 0.25 0.4259965 0.0 0.0 7.16846e-4
#integrator Newmark 0.5 0.25   0.4259965   0.0   0.0   7.16846e-4

```
algorithm Newton
#algorithm FHT

numberer Plain
system BandGeneral

analysis Transient
#analysis FHT

analyze 80 0.05
```

13 Appendix B: OpenSees Input Files for MR Damper FHT and Level 1 Simulations

Single Column Benchmark Model

```
#
#        This is a tcl and fht script file the first MR Damper benchmark
#        structure.  A single column is fully fixed at the base and attached
#        to a horizonally oriented damping element at the top.  With minor
#        changes this script can be modified to
#
#                1.  Run as a tcl input script for the standard release of OpenSees
#                2.  Run as a fht input script for the RT version of OpenSees developed
#                        at the CU Boulder FHT NEES laboratory
#                3.  A fully linear model
#                4.  A nonlinear model
#
#        These changes are easily made by altering the commenting of the appropriate
#        lines below
#
#
#        Modified 11-05-2007   EJS
#
#        MR Damper Benchmark Tests - Benchmark Structure #1
#
#        Single column of SAC Structure w/ Single MR Damper
#
# Units - kip, inch

#model FHT -ndf 3 -ndm 2
model BasicBuilder -ndf 3 -ndm 2

# define nodes for simple 1 column model
#        node#  x-coord          y-coord
node   1       0.0     0.0
node   2       0.0     52
node   3       360     52

# define nodal masses
#        node#  xMass           yMass  RotMass
mass   2       5.920875        1.0     1.0e-4
```

```
# define boundary conditions
#        node#  x      y       rotation
fix      1      1      1       1
fix      3      1      1       1

# Some material definitions
uniaxialMaterial Steel01        1 50 29000 1e-6
uniaxialMaterial Steel01        11 36 29000 1e-6


#                               mat#   C      exponent
uniaxialMaterial Viscous        2      214.3  1
# these properties are used to create a material for a truss element that
# can be used to represent a purely linear (viscous) MR Damper.  The value
# of C above is calculated using C=L*Cd/A where
#        L=length the truss element in inches [360]
#        Cd=viscous damping value taken from the standard EOM (m*a + Cd*v + k*x=f)
[Cd=45]
#        A=the x-section area of the truss element [75.6]


# This truss element w/ viscous material can be used to represent a linear MR damper
#               id#    nodeI  NodeJ  A       MaterialTag
element truss 2        2      3      75.6    2
#element                id#  node1  node2   actuator#  Ki   Ci   Ta2u  Tu2a  Fa2u
ForceMultiplier
#element ExperimentalElementTruss 2  2      3      3          0    45.0 1    1     1     1


#Column
geomTransf Linear 1

#                       ele#  nodeI  nodeJ  A       E      I       Transform
# element elasticBeamColumn 1      1      2       75.6    29000 3400    1
#  W14x257

#W14*257
section Fiber 20 {
patch   quad 11 3 2     -8.19  7.9975 -8.19 -7.9975    -6.3 -7.9975 -6.3 7.9975
patch   quad 11 1 5     -6.3   0.5875 -6.3  -0.5875     6.3 -0.5875 6.3  0.5875
patch   quad 11 3 2      6.3   7.9975  6.3  -7.9975     8.19 -7.9975 8.19 7.9975
}

#W14*311
section Fiber 21 {
patch   quad 11 3 2     -8.56  8.115  -8.56 -8.115     -6.3 -8.115  -6.3 8.115
patch   quad 11 1 5     -6.3   0.705  -6.3  -0.705      6.3 -0.705  6.3  0.705
```

```
patch   quad 11 3 2      6.3  8.115   6.3  -8.115      8.56 -8.115   8.56  8.115
}

#                EleTag  NodeI  NodeJ  NumIntPts  SecTag  TransTag
element nonlinearBeamColumn 1    1     2      4         20      1

puts "eigen values prior to transient analysis: [eigen 2]"


#recorder Node -time -scram -node 2 -dof 1 2 3 disp
#recorder Node -time -scram -node 2 -dof 1 2 3 vel
#recorder Node -time -scram -node 2 -dof 1 2 3 accel
recorder Node -file BM5ai_disp.out -time -node 2 -dof 1 2 3 disp
recorder Node -file BM5ai_vel.out -time -node 2 -dof 1 2 3 vel
recorder Node -file BM5ai_accel.out -time -node 2 -dof 1 2 3 accel
#recorder  RealTimeNode  DispRealTimeEBeams.out  disp  -time  -node  5  6  -dof  1  -
numStep 4000  #Use -numStep>=analysis time steps
#recorder  ElementPostAnalysis  1  -time    -file  validationEle.out  -numStep  1500
globalForce  #Use -numStep>=analysis time steps


# select a ground motion for input
pattern UniformExcitation 1 1 -accel "Path -filePath Elcentro1.txt -dt 0.01 -factor 386.4"


#converge test
#              tol     maxIter  printFlag
test EnergyIncr  1.0e-20    20       3
constraints Plain

#                      gammabeta    alphaM        betaK   betaKinit betaKcomm
integrator Newmark   0.5     0.25    0.46173 0.0  0.0  0.00037947
#integrator FHT      0.5     0.25    0.46173 0.0  0.0  0.00037947

algorithm Newton
#algorithm FHT

numberer Plain
system BandGeneral

analysis Transient
#analysis FHT

analyze 6800  0.01
```

Two Story Two Bay Benchmark Model

```
#
#        This is a tcl and fht script file the second MR Damper benchmark
#        structure.  A 2 story 2 bay frame that is fully fixed at the base and attached
#        to a horizonally oriented damping element at the top of the 1st story center
#        column.  With minor changes this script can be modified to
#
#                    1.  Run as a tcl input script for the standard release of OpenSees
#                    2.  Run as a fht input script for the RT version of OpenSees developed
#                           at the CU Boulder FHT NEES laboratory
#                    3.  A fully linear model
#                    4.  A nonlinear model
#
#        These changes are easily made by altering the commenting of the appropriate
#        lines below
#
#
#        Modified 11-05-2007   EJS
#
#        Units: kip, in, sec
#
#
#   @_____@|@_____@|
# 03         06         09
# |          |          | 156"
# |          |          |
# |@_____@|@_____@|
# 02         05         08
# |          |          | 156"
# |          |          |
# 01         04         07
#      360"        360"


#model FHT -ndm 2 -ndf 3
model BasicBuilder -ndm 2 -ndf 3


#   tag   X     Y
node  10       0
node  20       156
node  30       312

node  4360     0
node  5360     156
```

node 6360   312

node 7720   0
node 8720   156
node 9720   312

node   DX   DY   RZ
fix   1   1   1   1
fix   4   1   1   1
fix   7   1   1   1

uniaxialMaterial Steel01 4   1.7933E+4   171100000 0.0000005
uniaxialMaterial Steel01 5   1.6433E+4   142970000 0.0000005
uniaxialMaterial Steel01 6   7.7215E+3   53070000 0.0000005

Define material for pined-pined beams
uniaxialMaterial Elastic 10 29000

uniaxialMaterial Steel01 11 36 29000 1e-6

section Uniaxial 11 4 Mz
section Uniaxial 12 5 Mz
section Uniaxial 13 6 Mz

Coordinate transformation
#geomTransf PDelta 1
geomTransf Linear 1
geomTransf Linear 2

Define column elements of the structure
idtag ndI   ndJ   A   E   I   transfTag
#element elasticBeamColumn 1   1   2   75.6 29000 3400   1
#element elasticBeamColumn 2   4   5   91.4 29000 4330   1
#element elasticBeamColumn 3   7   8   91.4 29000 4330   1

#element elasticBeamColumn 4   2   3   75.6 29000 3400   1
#element elasticBeamColumn 5   5   6   91.4 29000 4330   1
#element elasticBeamColumn 6   8   9   91.4 29000 4330   1

#W14*257

```
section Fiber 20 {
patch   quad 11 3 2    -8.19  7.9975  -8.19  -7.9975    -6.3  -7.9975  -6.3  7.9975
patch   quad 11 1 5    -6.3   0.5875  -6.3   -0.5875    6.3  -0.5875  6.3  0.5875
patch   quad 11 3 2     6.3   7.9975   6.3   -7.9975    8.19 -7.9975  8.19  7.9975
}

#W14*311
section Fiber 21 {
patch   quad 11 3 2    -8.56  8.115   -8.56  -8.115     -6.3  -8.115  -6.3  8.115
patch   quad 11 1 5    -6.3   0.705   -6.3   -0.705     6.3  -0.705  6.3  0.705
patch   quad 11 3 2     6.3   8.115    6.3   -8.115     8.56 -8.115  8.56  8.115
}


#                   EleTag  NodeI  NodeJ  NumIntPts  SecTag  TransTag
element nonlinearBeamColumn 1    1    2     4       20      2
element nonlinearBeamColumn 2    4    5     4       21      2
element nonlinearBeamColumn 3    7    8     4       20      2

element nonlinearBeamColumn 4    2    3     4       20      2
element nonlinearBeamColumn 5    5    6     4       21      2
element nonlinearBeamColumn 6    8    9     4       20      2



# Define nonlinear beam elements of the structure in fixed-fixed bays
#                 idtag ndI ndJ  SecTag Lpi  SecTag Lpj  E    A    I    transfTag
element beamWithHinges    7  2  5  11   0.1   11    0.1 29000 34.7 5900  1
element beamWithHinges    8  5  8  11   0.1   11    0.1 29000 34.7 5900  1

element beamWithHinges    9  3  6  12 0.1  12 0.1 29000 34.2 4930  1
element beamWithHinges   10  6  9  12 0.1  12 0.1 29000 34.2 4930  1

# Define linear beam elements of the structure in fixed-fixed bays
#                 idtag ndI ndJ  A    E      I      transfTag
#element elasticBeamColumn   7  2  5   34.7 29000  5900    1
#element elasticBeamColumn   8  5  8   34.7 29000  5900    1

#element elasticBeamColumn   9  3  6   34.2 29000  4930    1
#element elasticBeamColumn  10  6  9   34.2 29000  4930    1



#                          mat#   C      exponent
uniaxialMaterial Viscous     2      233.5  1
# these properties are used to create a material for a truss element that
# can be used to represent a purely linear (viscous) MR Damper.  The value
```

# of C above is calculated using C=L*Cd/A where
#   L=length the truss element in inches [392.35]
#   Cd=viscous damping value taken from the standard EOM (m*a + Cd*v + k*x=f)
[Cd=45]
#   A=the x-section area of the truss element [75.6]

#element sNodeElement 11 5 1 1 1 1 1 1 1 131.19 0 4135.83 0 967.65 0 4135.83 0
204128.4 1 0 0 0 -0.5 -0.5 0 0.01389 -0.01389 1 0 0 0 -1 36 0 -1 -36
This truss element w/ viscous material can be used to represent a linear MR damper
ele#   nodeI   NodeJ A   MaterialTag
element truss 11   5   7   75.6   2

#element   id node1   node2   actuator# Ki Ci Ta2u Tu2a Fa2u
ForceMultiplier
#element ExperimentalElementTruss 11   5   7   3   0 45.0 1   1   1   1

# Create gravity loads
pattern Plain 1 Constant {
load   2   0   -22.00333333 0.0
load   5   0   -44.00666667   0.0
load   8   0   -22.00333333 0.0

load   3   0   -23.81458333 0.0
load   6   0   -47.62916667   0.0
load   9   0   -23.81458333 0.0

}

Add mass as lumped mass with no (very little) roational inertia
node   mx   my   mrot

mass 2   0.341665   0.05694417   2.10856e-4
mass 5   0.68333   0.113888   4.21712e-4
mass 8   0.341665   0.05694417   2.10856e-4

mass 3   0.36979165   6.163194e-2   228.214275429
mass 6   0.7395833   0.12326388   456.428550857
mass 9   0.36979165   6.163194e-2   228.214275429

#puts "eigen values prior to transient analysis: [eigen 3]"

system BandGeneral
constraints Plain

test NormDispIncr 1.0e-8 10

#algorithm FHT
algorithm Newton

numberer Plain

4% damping modes 1&3: integrator   Newmark 0.5   0.25   0.800623   0.0   0.0   0.000815647
#integrator FHT 0.5 0.25 0.800623 0.0 0.0 0.000815647
integrator Newmark 0.5 0.25 0.800623 0.0 0.0 0.000815647

#analysis FHT
analysis Transient

input and scale base motion record
pattern UniformExcitation 2 1 -accel "Path -filePath Elcentro1.txt -dt 0.01 -factor 386.4"

recorder Node -file BM5bi_disp.out -time -node 5 2 3 -dof 1 disp
recorder Node -file BM5bi_vel.out -time -node 5 2 3 -dof 1 vel
recorder Node -file BM5bi_accel.out -time -node 5 2 3 -dof 1 accel
#recorder Node -time -scram -node 2 -dof 1 2 3 disp
#recorder Node -time -scram -node 2 -dof 1 2 3 vel
#recorder Node -time -scram -node 2 -dof 1 2 3 accel
#recorder Node -time -scram -node 3 -dof 1 2 3 disp
#recorder Node -time -scram -node 3 -dof 1 2 3 vel
#recorder Node -time -scram -node 3 -dof 1 2 3 accel
#recorder Node -time -scram -node 5 -dof 1 2 3 disp
#recorder Node -time -scram -node 5 -dof 1 2 3 vel
#recorder Node -time -scram -node 5 -dof 1 2 3 accel

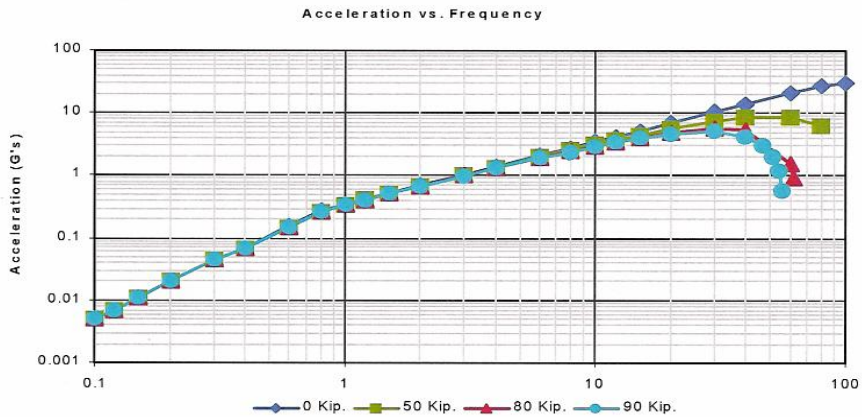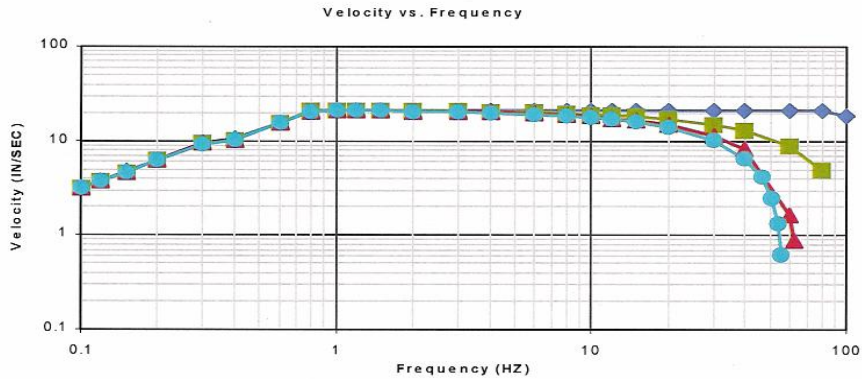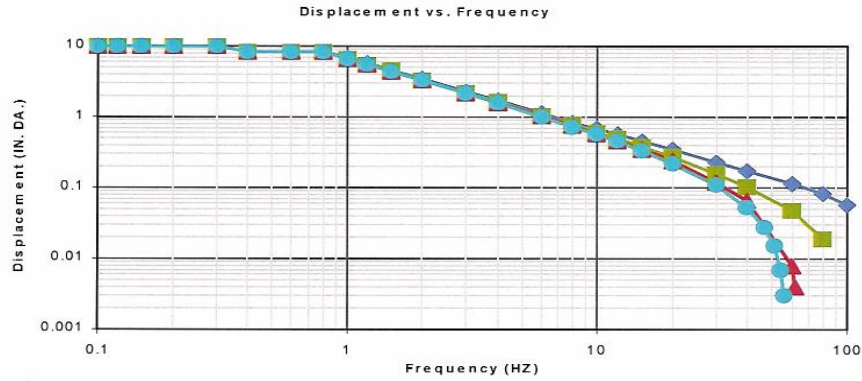analyze   6800   0.009766

14 Appendix C: MTS Actuator Performance Curves

System Performance Curves

Customer	University of Colorado	Date Created	7/7/01 23:42
Prepared By	Ray Sydeski		

Displacement vs. Frequency

Velocity vs. Frequency

Acceleration vs. Frequency

Legend: 0 Kip. — 50 Kip. — 80 Kip. — 90 Kip.

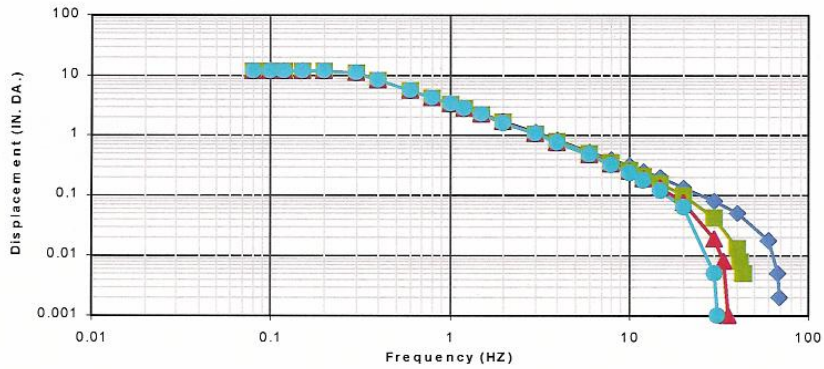| Pump		Servovalve		Actuator	
Model:	506.81	Model:	256.18A02	Model:	244.41str
Nominal Rating:	140 GPM	Nominal Rating:	180 GPM	Nominal Rating:	111 Kip
System Pressure:	3000 PSI.	Quantity:	1	Stroke:	10 IN.

The plots above represent a mathematical prediction of system performance. Possession of this information is not a guarantee that a system will perform as predicted. MTS will not be liable for any incidental or consequential damages or losses arising from use of this information. Interpretation of the data and its use are the sole responsibility of the user.
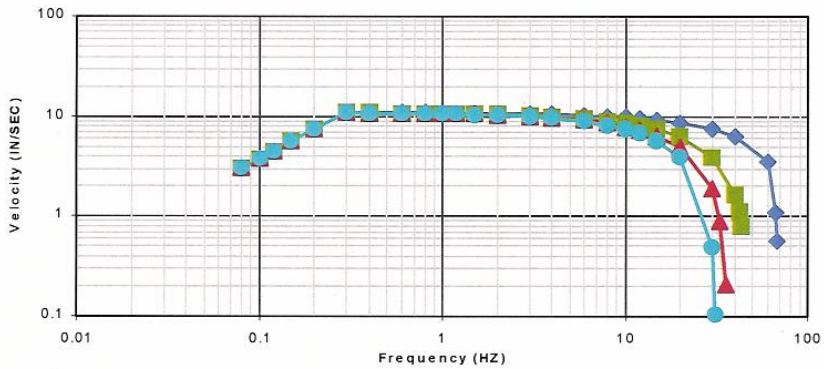
System Performance Curves

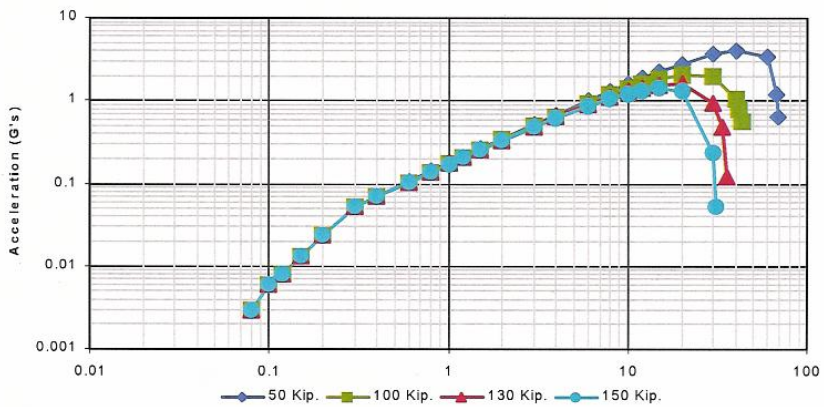| Customer	University of Colorado	Date Created	7/7/01 23:32
Prepared By	Ray Sydeski		

Displacement vs. Frequency

Velocity vs. Frequency

Acceleration vs. Frequency

50 Kip. — 100 Kip. — 130 Kip. — 150 Kip.

Pump		Servovalve		Actuator	
Model:	506.81	Model:	256.25A02	Model:	244.51str
Nominal Rating:	140 GPM	Nominal Rating:	250 GPM	Nominal Rating:	219 Kip
System Pressure:	3000 PSI.	Quantity:	1	Stroke:	12 IN.

The plots above represent a mathematical prediction of system performance. Possession of this information is not a guarantee that a system will perform as predicted. MTS will not be liable for any incidental or consequential damages or losses arising from use of this information. Interpretation of the data and its use are the sole responsibility of the user.

[1] Wallen, R. "SCRAMNet LabVIEW Data Acquisition System", CU-NEES-07-16 Technical Report., 2007

[2] Shing, P.B., Vannan, M.T., and Carter, E., "Implicit time integration for pseudodynamic tests", *Earth. Engrg, and Struct. Dynamics*, Vol. 20, 1991, 551-576.

[3] H.M. Hilber, T.J.R. Hughes and R.L. Taylor, "Improved numerical dissipation for time integration algorithms in structural dynamics", Earthquake eng. Struct. Dyn. 5, 283-292 (1977).

[4] Hughes, T.J.R., "Analysis for transient algorithms with particular reference to stability behavior", Belyschko T, Hughes TJR, Editors. *Computational methods for transient analysis*. Amsterdam, North-Holland, 1983.

[5] Shing, P.B., Spacone, E. and Stauffer, E. Conceptual design of fast hybrid test system at the University of Colorado. Proceeding, Seventh U.S. National Conference of Earthquake Engineering, Boston.

[6] Taucer, Fabio F, E Spacone, FC Filippou. A Fiber Beam-Column Element for Seismic Response Analysis of Reinforced Concrete Structures. Report No. UCB/EERC-91/17 (http://nisee.berkeley.edu/elibrary/getdoc?id=237794). Earthquake Engineering Research Center, College of Engineering, University of California, Berkeley. December 1991.

[7] Scott, M.H. and G.L. Fenves. "Plastic Hinge Integration Methods for Force-Based Beam-Column Elements", Journal of Structural Engineering, ASCE, 132(2):244-252, February 2006.

[8] Spencer, B.F., Jr., Dyke, S. J., Sain, M.K., and Carlson, J. D. (1997). "Phenomenological Model of a Magnetorheological Damper," *Journal of Engineering Mechanics, ASCE*, Vol. 123, No. 3, pp. 230 238.

[9] Gavin, H.P. (2001). "Multi-Duct ER Dampers." *Journal of Intelligent Material Systems and Structures*, Vol. 12, No. 5, pp.353-366.

[10] Houriuchi, T., Inoue, M., Konno, T., Namita Y., Real-time hybrid experimental system with actuator delay compensation and its application to a piping system with energy absorber, Earthquake Engineering and Structural Dynamics, 28, 1121-1141, 1999.

[11] Somerville, P., Smith, N., Punyamurthula, S., Sun, J., Development of Ground Motion Time Histories for Phase 2 of the FEMA/SAC Steel Project & Other Reports available from CUREE, Draft Report Woodward-Clyde Federal Services, Pasadena, California, March 1997.

[12] Mosqueda, G., Stojadinovic, B., and Mahin, S. Implementation and accuracy of continuous hybrid simulation with geographically distributed substructures. Report No. EERC 2005-02 Earthquake Engineering Research Center, College of Engineering, University of California, Berkeley. November 2005.